



# Quaternary interaction of cryospheric and oceanographic processes along the central-east Greenland margin

LARA F. PÉREZ , TOVE NIELSEN, TINE L. RASMUSSEN AND MONICA WINSBORROW

BOREAS



Pérez, L. F., Nielsen, T., Rasmussen, T. L. & Winsborrow, M. 2019 (January): Quaternary interaction of cryospheric and oceanographic processes along the central-east Greenland margin. *Boreas*, Vol. 48, pp.72–91. <https://doi.org/10.1111/bor.12340>. ISSN 0300-9483.

The east Greenland margin has been influenced by oceanographic and cryospheric processes since the late Miocene, when the southwards flow of the East Greenland Current (EGC) initiated and ice sheets first advanced across the margin. However, the relative importance of these processes, and their influence on the sedimentation of the margin through time remains poorly understood. High-resolution single-channel seismic, chirp sub-bottom profiles and swath bathymetry data were acquired along the middle/lower slope and proximal basinal area off Liverpool Land, central-east Greenland margin. In this study, seismic-stratigraphical and morphological analyses allowed us to distinguish between the major sedimentary processes that influenced this margin during the Quaternary. The stratigraphical architecture reveals mass transport deposits (MTDs) related to glacially influenced down-slope sedimentation. These are intercalated with buried contourite systems associated with bottom-current controlled along-slope sedimentation. The distribution of the MTDs suggests the influence of two distinct ice-stream systems. Initial phases of down-slope deposition during the early-middle Quaternary appears to be related to distal deposition fed by an ice stream from the Scoresby Sund area in the south. Shallow sedimentary processes, together with morphological analysis of the sea floor, show that the most recent activity of down-slope processes during the latest Quaternary has occurred in the north, linked to an ice stream from the Kong Oscar Fjord area. These observations document a temporal shift in the relative dominance of the Scoresby Sund and Kong Oscar Fjord ice-stream systems. The glacial influence on the margin has been interrupted by periods of stronger activity of along-slope bottom-current flow, demonstrating that the EGC periodically controlled sedimentation on the continental margin.

Lara F. Pérez ([lfp@geus.dk](mailto:lfp@geus.dk); [larafperez@gmail.com](mailto:larafperez@gmail.com)) and Tove Nielsen, Department of Geophysics, Geological Survey of Denmark and Greenland (GEUS), Øster Voldgade 10, Copenhagen DK-1350, Denmark; Tine L. Rasmussen and Monica Winsborrow, Department of Geosciences, Centre for Arctic Gas Hydrate, Environment and Climate University of Tromsø (UiT) – The Arctic University of Norway, Tromsø N-9037, Norway; received 26th February 2018, accepted 9th July 2018.

Since the mid-Pliocene onset of large-scale Northern Hemisphere glaciation, the cryospheric and oceanographic evolution of the Greenland margins is considered to have followed the glacial–interglacial cycles of the Quaternary (e.g. Sarnthein *et al.* 2009). The impact of the Greenland Ice Sheet on the adjacent continental margins has been addressed in several works (e.g. Larsen *et al.* 1994; Hubberten *et al.* 1995; Swift *et al.* 2008; Thiede *et al.* 2010; Nielsen & Kuijpers 2013; Knutz *et al.* 2015; Laberg *et al.* 2018; Pérez *et al.* 2018), in particular the evolution, at different scales, of the ice streams that flowed through the major fjords and cross-shelf troughs (e.g. Stein *et al.* 1993; Solheim *et al.* 1998; Evans *et al.* 2002; Ó Cofaigh *et al.* 2003; Berger & Jokat 2009; Laberg *et al.* 2013). Other works have focused on the interaction between glacigenic debrisflows (GDFs) and hemipelagic sedimentation (e.g. Butt *et al.* 2001) or deep sea channel formation (e.g. Wilken & Mienert 2006). However, most of the regional works are largely focused on the late Quaternary evolution of the Greenland Ice Sheet (e.g. Stein *et al.* 1996; Håkansson *et al.* 2007; Thiede *et al.* 2010; Zhuravleva *et al.* 2017).

The Quaternary oceanographic evolution of the northern North Atlantic is generally understood (Fig. 1A), including the present oceanographic pattern of the Greenland Sea (e.g. Wolf & Thiede 1991; Sarnthein &

Altenbach 1995; Sarnthein *et al.* 2009; Våge *et al.* 2013; Håvik *et al.* 2017). The vertical water-column structure of the North Atlantic Ocean has experienced little variation over the Quaternary, despite the dramatic climatic shifts (Raymo *et al.* 2004). However, variations did occur in the northwards advection of oceanic heat, in the meltwater input from the Greenland Ice Sheet and in the inflow and outflow waters through the surrounding straits with a reduction in North Atlantic Deep Water (NADW) formation during the Last Glacial Maximum (LGM) (Marchitto *et al.* 2002; Raymo *et al.* 2004; Zachos *et al.* 2008; Zhuravleva *et al.* 2017).

Detailed seismo-stratigraphical studies of the interaction between cryospheric and oceanographic changes and their respective effect on the sedimentary processes have been carried out along the western (Nielsen & Kuijpers 2013; Knutz *et al.* 2015) and southeastern (Clausen 1998; Rasmussen *et al.* 2003) Greenland margins, and lately along the central-east Greenland margin (Pérez *et al.* 2018) from a large-scale perspective. The present work however combines results from high-resolution seismic and sub-bottom profiles, swath bathymetry and gravity cores collected along the continental slope offshore central-east Greenland (Fig. 1). The aim of this work is to reveal the Quaternary evolution of the central-east Greenland margin based on the detailed

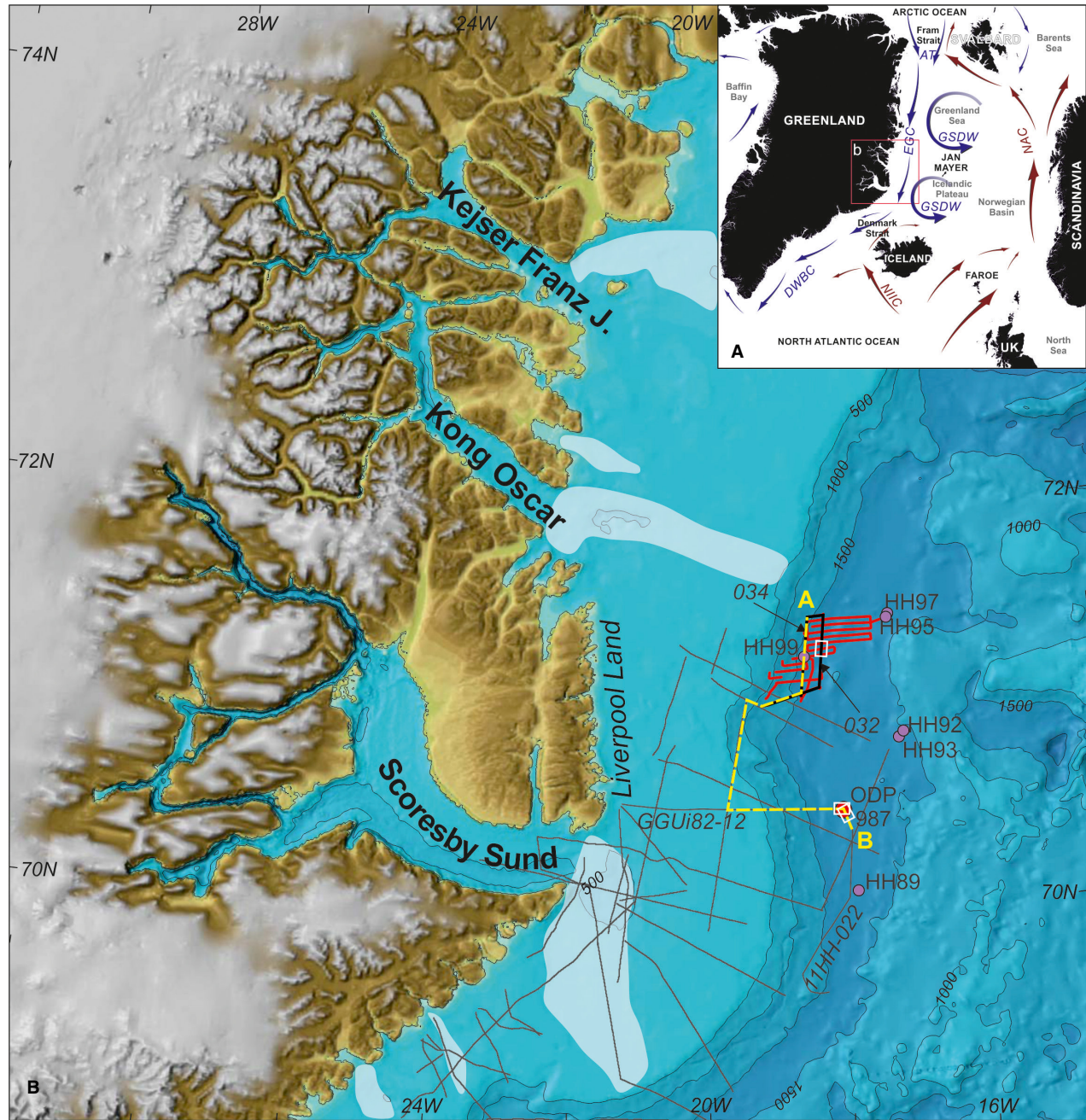


**Fig. 1.** Regional setting of the study area. A. Oceanographic framework of the North Atlantic Ocean based on Wolf & Thiede (1991) and Våge *et al.* (2013). Major boundary currents are represented, distinguishing between warm (red) and cold (blue) flows: AT = Arctic Throughflow; EGC = East Greenland Current; GSDW = Greenland Sea Deep Water; NAC = Norwegian Atlantic Current; and Deep Western Boundary Current (DWBC) and North Icelandic Irminger Current (NIIC) as part of the Atlantic Meridional Overturning Circulation (AMOC). B. Bathymetric map of the study area based on the International Bathymetric Chart of the Arctic Ocean (IBCAO, Jakobsson *et al.* 2012). Isobaths every 500 m. Major troughs shaded in white. Location of the data used in this work: red lines = tracks of the chirp sub-bottom profiles; black lines = single-channel seismic profiles (notice the location of profiles CAGEAO13\_034 (034) and CAGE\_OA2013-032 (032) shown in Figs 7 and 8, respectively). The white squares mark the location of the seismic sections shown in Fig. 3. The location of multi-channel seismic profiles connecting ODP 987 (red dot) with the study area is shown in grey. The seismic correlation shown in Fig. 2 is marked in yellow as profile A–B. The gravity cores available in the study area are shown as purple dots. [Colour figure can be viewed at [www.boreas.dk](http://www.boreas.dk)]

mapping of the glacial-related and current-related features and deposits within the study area. The main goal is to identify the relative importance of the Greenland Ice Sheet and bottom-current influ-

ence on the development of the central-east Greenland slope, i.e. the interactions between the cryospheric and oceanographic processes, during the Quaternary.

## Regional framework

The study area is located oceanwards of the continental shelf edge, in the slope and proximal basinal area off Liverpool Land on the central-east Greenland margin (Fig. 1). Although the Liverpool Land margin constitutes a passive margin, uplift occurred most recently during the early Pliocene, influencing ice-sheet behaviour (Japsen *et al.* 2014; Døssing *et al.* 2016). Glaciations have played an important role in the building of the margin. Several major ice streams have operated on the continental shelf, carving cross-shelf troughs and depositing large prograding wedges forming trough-mouth-fans (TMFs; e.g. Vorren & Laberg 1997; Berger & Jokat 2009), both common elements along high latitude margins (e.g. Nielsen *et al.* 2005). The Greenland Ice Sheet history started during the Eocene/Oligocene with a succession of cooling events before a major intensification of glaciations during the Pliocene/Pleistocene (Larsen *et al.* 1994; Solheim *et al.* 1998; Tripati *et al.* 2008). The most recent major advances of the Greenland Ice Sheet across the eastern shelf occurred during the Saalian glaciation (0.20–0.13 Ma; Vanneste *et al.* 1995; Solheim *et al.* 1998; Håkansson *et al.* 2007) and the LGM (Evans *et al.* 2002; Ó Cofaigh *et al.* 2002, 2004). In addition to these large-scale glaciations, several local glaciations have been documented along the central-east Greenland margin, such as the Scoresby Sund glaciation from 0.24 to 0.13 Ma and the Flakkerhuk glaciation from 0.06 to 0.01 Ma (Funder *et al.* 1994, 1998).

The present-day oceanographic pattern of the study area is dominated by the southwards flow of the East Greenland Current (EGC; e.g. Våge *et al.* 2013). The evolution of this current has mainly been determined by the tectonic formation of the Fram and Denmark Straits (Fig. 1A). The Fram Strait represents the main connection between the Arctic Ocean and the Greenland Sea, whereas the Denmark Strait connects the Greenland Sea with the North Atlantic (Fig. 1A). The exact timing of the opening of the Fram Strait, as well as the generation of the deep-water oceanic connection, remains unresolved. The proposed opening time ranges from the Oligocene to the Miocene/Pliocene boundary (e.g. Engen *et al.* 2008; Ehlers & Jokat 2013; Mattingdal *et al.* 2014). The overflow of deep water from the Greenland Sea (mainly formed by Northern Component Water) through the Denmark Strait began during the early Miocene (Wright & Miller 1996; Engen *et al.* 2008; Ehlers & Jokat 2013), but it may periodically have been restricted by tectonic pulses along the Greenland-Scotland Ridge (Wright & Miller 1996; Poore *et al.* 2006; Parnell-Turner *et al.* 2015). The onset of flow of the EGC along the east Greenland margin is suggested to have occurred around 8.3 Ma (Wolf & Thiede 1991; Våge *et al.* 2013). Since then, the flow of the EGC has been influenced by the glacial–interglacial fluctuations, which changed the position of the Arctic Front and, as a

consequence, the areal distribution of the water-masses involved in the flow (e.g. Mokeddem & McManus 2016). During southward advances of the Arctic Front, convection increases, enhancing polar heat transport and favouring expansion of Northern Hemisphere ice sheets (e.g. Mokeddem & McManus 2016). At present, the EGC flow off Liverpool Land comprises several water-masses occupying distinct depths in the water column. The Polar Water occupies the continental shelf shallower than 200 m (Aagaard & Coachman 1968); the Return Atlantic Current (RAC) carries Atlantic Intermediate Water between 150 and 800 m (Hopkins 1991); while the lower continental slope and basinal area are influenced by the Greenland Sea Deep Water (GSDW), generated by convection in the Greenland Sea (Hopkins 1991; Jeansson *et al.* 2008).

## Data and methods

### Database

The data set used in this work consists of swath bathymetry, chirp sub-bottom profiles and high-resolution single-channel seismic data (Fig. 1B). The data were obtained in 2013 onboard the RV ‘Helmer Hanssen’ led by the Department of Geosciences at University of Tromsø (UiT) – the Arctic University of Norway – and the Centre for Arctic Gas Hydrate, Environment and Climate (CAGE). The swath bathymetry was acquired with a Kongsberg Maritime EM300 multibeam and EK60 split-beam (18, 38 and 120 kHz) echo sounders covering both deep and shallow water depths over an area of 1500 km<sup>2</sup>. Sound velocity profiles of the water column were acquired for calibration. Preliminary processing of the multibeam data was performed using Neptune software, while post-processing was done with Fledermaus software. DMagic software was used to generate grids with 30 m cell size. Visualization and interpretation of these data were carried out using Fledermaus and ArcGIS software. Chirp sub-bottom profiles, with a total length of 1004 km, were obtained simultaneously with the multibeam data (Fig. 1B). The acquisition system was a hull-mounted EdgeTech 3300-HM sub-bottom profiler operating at 3.5 kHz. Pulse mode and shot rate were varied depending on the water depth. The maximum penetration is 35–40 ms two-way-travel-time (TWTT) and was obtained in the southern part of the study area.

Four high-resolution single-channel seismic profiles, with a total length of 155 km, were acquired on the lower slope, and at the base of the slope within the study area (Fig. 1B). The seismic source was a single Sercel GI mini airgun of 45 cubic inches and the receiver was a single-channel streamer of 6 m active section with 20 hydrophones. The sampling rate was 0.5 ms. Post-processing of the seismic data followed a normal sequence of single-channel processing. The seismic penetration allows a

detailed analysis down to 0.4 s TWTT below the sea floor and identification of major seismic features to about 1 s TWTT below the sea floor. Interpretation of the sub-bottom and seismic profiles was carried out using Petrel software, following conventional seismic stratigraphical analysis (e.g. Payton 1977).

#### *Age estimation*

The age model of the major seismic units identified in the present study is adapted from a newly established stratigraphical framework for the central-east Greenland margin (Pérez *et al.* 2018). This work presents a reconstruction of the central-east Greenland margin since Miocene times, providing an estimated age of the mapped stratigraphical discontinuities by correlation with Site 987 of ODP Leg 162 located in the basinal area off Scoresby Sund (Jansen *et al.* 1996; Channell *et al.* 1999; Pérez *et al.* 2018). The ODP 987 region is connected to the central-east Greenland margin by a network of seismic profiles (Fig. 1B). A comparison of the large-scale seismic patterns of these seismic lines with those of the present study allows correlation of the two upper units of the stratigraphical model presented in Pérez *et al.* (2018) to the seismic network of this work as shown in Fig. 2. Thus, according to the chronological model, the age of the lower seismic unit of the present work, seismic unit U2 (see below), is assigned to the early Pleistocene. The base of U2 is formed by a regional stratigraphical discontinuity Discontinuity-b of an estimated age of 2.05 Ma (Pérez *et al.* 2018). The age of the upper seismic unit of the present study, seismic unit U1 (see below), is assigned to the early-middle Pleistocene-Holocene. The top of U1 is defined by the sea floor and therefore considered to represent 0 Ma, and the base of the unit is formed by the seismic Discontinuity-a of Pérez *et al.* (2018) (Figs 2, 3). The age of Discontinuity-a was estimated to 1.6 Ma and thus correlates with the age of seismic reflector R1 of earlier chronostratigraphical models of the ODP site 987 (Jansen *et al.* 1996; Channell *et al.* 1999). In the present study, U1 was divided into subunits (see below), which could also be recognized, based on the affinity of seismic facies, on two seismic profiles of the regional age model (GGUi82-12 and 11HH-GEO8144-022; Fig. 1B) and could thus be tied to ODP 987 for an approximate age estimation using linear interpolation (Fig. 3; Jansen *et al.* 1996; Butt *et al.* 2001; Laberg *et al.* 2013; Pérez *et al.* 2018).

During the 2013-expedition several gravity and piston cores were recovered in the study area (Fig. 1B). Gravity core HH13-099GC is located over line CAGE-OA2013-034, recovering 5.41 m of sediments at 1550 m water depth. The average sound velocity in the sediments is  $1579.17 \text{ ms}^{-1}$  measured in the core. The magnetic susceptibility profile of this core is similar to the curves of gravity cores HH13-089GC and HH13-092GC located in the basinal area to the SE of the study area

and to other core records from the central-east Greenland margin with very similar  $^{14}\text{C}$  ages, depositional rates and oxygen isotope stratigraphy (see Stein *et al.* 1996) (Figs 1B, 4). Cores HH13-089GC (1616 m water depth; Gabrielsen 2017) and HH13-092GC (1595 m water depth) were accelerator mass spectrometry (AMS)  $^{14}\text{C}$  dated by monospecific samples of the planktonic foraminiferal species *Neogloboquadrina pachyderma*. The dates were calibrated to calendar years based on the Calib7.04, Marine13 program (Stuiver & Reimer 1993; Reimer *et al.* 2013) using the 405-year reservoir age correction inherent in the program, adding the regional correction  $\Delta R = 140 \pm 20$  (Hjort 1973). The identification of marine oxygen isotope stages (MIS) in core HH13-089GC is based on measurements of oxygen isotope values in the planktonic foraminiferal species *Neogloboquadrina pachyderma*, in combination with counts of ice-raftered debris and foraminifera (Fig. 4; Gabrielsen 2017). In core HH13-092GC, an age of 46.8 cal. ka is found at 2.05 m below the sea floor (Fig. 4). Using the age models from these gravity cores (Figs 1B, 4), and assuming a relatively stable sedimentation rate in the study area during the late Quaternary, the age of the base of the upper subunit can be estimated to c. 0.4 Ma, which agrees with the age estimated for this horizon from ODP 987 (Figs 3, 4).

#### *Terminology*

The morpho-sedimentary nomenclature used in this paper is clarified below. ‘Contourites’ refers to sediments deposited or substantially reworked by the persistent action of bottom currents (e.g. Stow *et al.* 2002; Rebescu 2005). This term thus includes a large array of sediments affected to varying degrees by different types of currents (Rebescu *et al.* 2014). Thick, extensive sedimentary accumulations are considered ‘contourite drifts’ or ‘drifts’. We adopted the contourite drift classification criteria from Faugères *et al.* (1999) and Rebescu (2005), identifying two main types of drifts: (i) the mounded drifts, which are mounded and elongated; and (ii) the sheeted drifts, which are represented by broad, tabular to slightly mounded geometries. A third type, usually called plastered drifts, has a morphology that lies between the two other types (e.g. Rebescu *et al.* 2014). Sediment waves are frequently associated with contourite drifts, expressed as transverse, asymmetrical bedforms of smaller dimensions. The crests of contourite-related sediment waves are slightly sinuous, with rare bifurcation and aligned perpendicular or oblique to the flow direction (Wynn & Stow 2002). Contourite-related sediment waves represent deposition under long-term stable current conditions at low flow velocities (Stow *et al.* 2002; Rebescu *et al.* 2014). In contrast, sediment waves related to across-slope flows show moderate sinuosity and regular bifurcation and are commonly found parallel to the slope or rise,

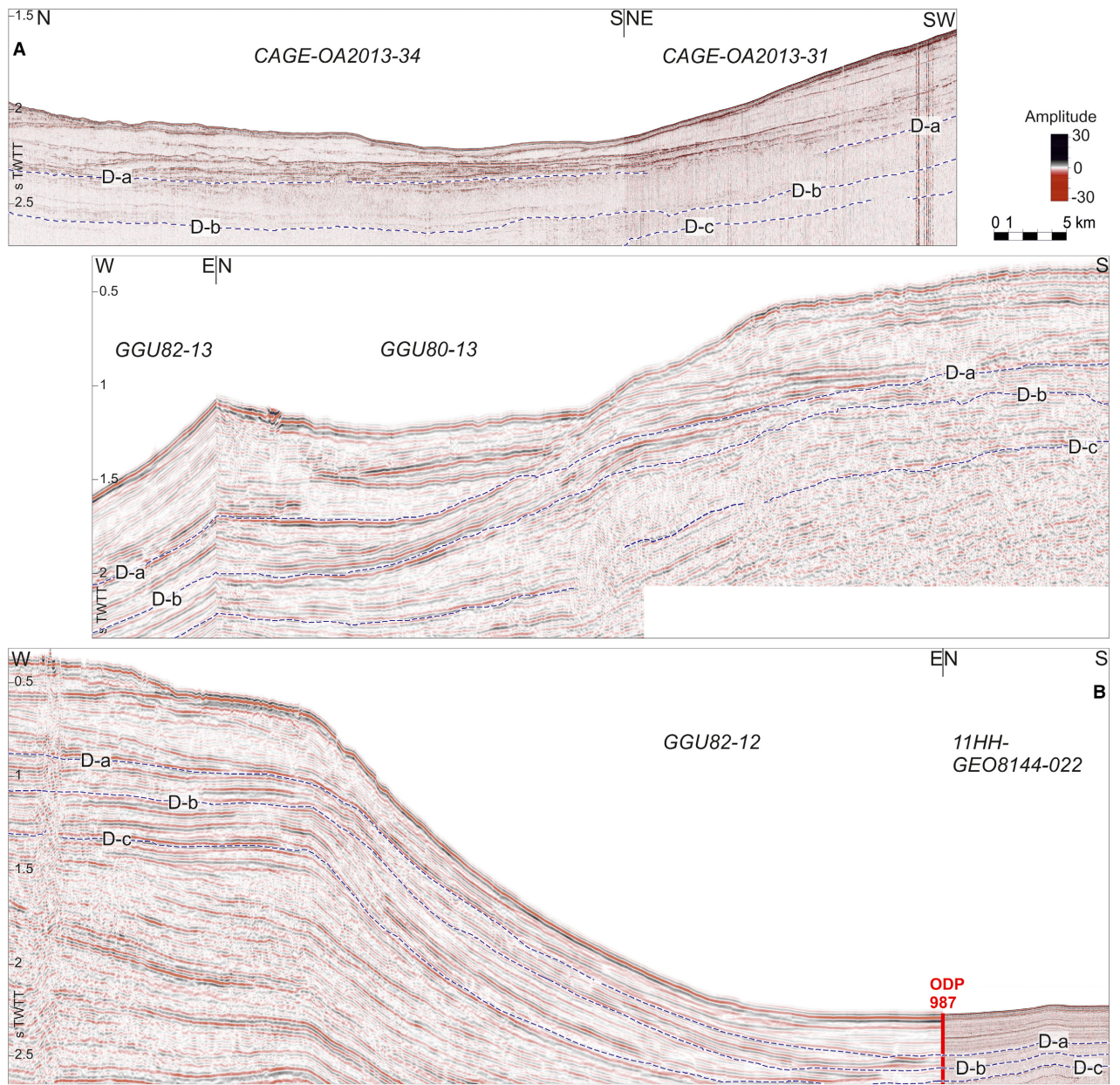


Fig. 2. Seismic correlation between the study area off Liverpool Land, and the ODP 987 off Scoresby Sund. Discontinuities a, b and c (D-a, D-b, D-c, respectively) are marked. Vertical scale in two-way-travel-time (TWTT). The location of the composite line is shown in Fig. 1 as profile A–B. [Colour figure can be viewed at [www.boreas.dk](http://www.boreas.dk)]

between channels or sedimentary lobes (Wynn & Stow 2002).

Mass transport deposits (MTDs) have collectively been identified as bodies with a transparent or semi-transparent seismic facies in which internal reflections may be locally observed (Reading 1996). Amongst the large variety of MTDs, GDF deposits are acoustically transparent or semi-transparent bodies that lack the chaotic and higher amplitude acoustic character of the larger slope failures such as sediment slides (Pickering & Hiscott 2016). The term ‘GDF system’ is used in this work for the combination of MTDs and channel-levees of

glacial origin (e.g. Laberg & Vorren 1995). Considering the vertical resolution of the seismic data (~3 m), individual MTDs could comprise several events undistinguishable at the seismic scale, and therefore, they could be considered as mass transport complexes as defined by Pickering & Hiscott (2016).

Pockmarks are nearly circular depressions formed where fluids escape through sea-floor sediment (Cathles *et al.* 2010). These imprints are common where gas is present in the near sea-floor sediments and are usually associated with other fluid migration structures such as chimneys or polygonal faults (Cathles *et al.*

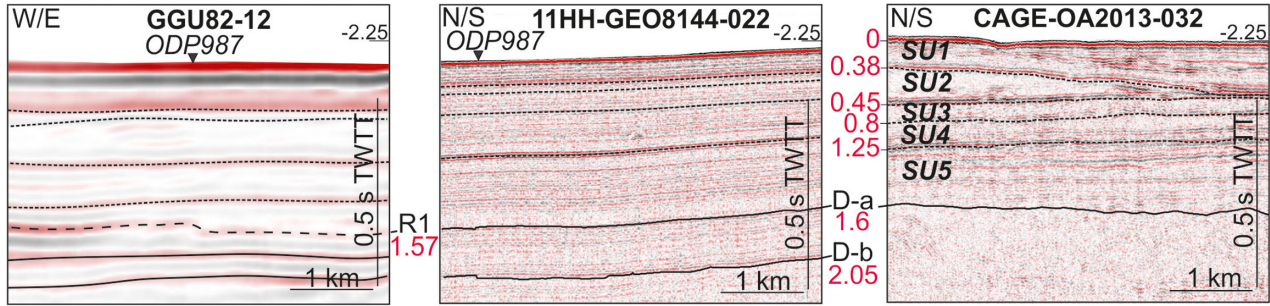


*Fig. 3.* Minor discontinuities (dotted black lines) in line CAGE\_OA2013-032 correlated with the lines GGU82-12 and 11HH-GEO8144-022 tie to ODP987 off Scoresby Sund (for locations, see Fig. 1). Vertical scale in two-way-travel-time (TWTT). D-a and D-b (black lines) correspond with the discontinuities described in Pérez *et al.* (2018), and R1 (dotted black line) corresponds with the local upper discontinuity identified in Channell *et al.* (1999) and Jansen *et al.* (1996) in the ODP site 987. Ages in Ma (in red). [Colour figure can be viewed at [www.boreas.dk](http://www.boreas.dk)]

2010). Pockmarks and fluid migration structures are identified in this work and mentioned as part of the margin description, but otherwise not further discussed.

## Results and interpretation

### Physiography

The study area is located off northern Liverpool Land where the continental shelf widens from 70 to 100 km from south to north (Fig. 1B). The continental shelf is generally over 200 m deep, deepening to 400 m at the shelf edge. It presents an irregular morphology marked by several cross-shelf troughs. The slope, about 30 km wide, passes into the basinal area of the southern and shallowest part of the Greenland Sea, with water depths over 1700 m (Fig. 1B).

The upper slope extends from 400 to 700 m water depth with gradients between 5° and 3°, being wider and gentler in the north. The swath bathymetry data extend from the middle slope to the adjacent basinal area where the depth varies between 650 and 1770 m below sea level (Figs 1B, 5). The middle slope is characterized by gradients ranging from 4° in the south to 2° in the north, while the lower slope is gentler with gradients of 2° in the south and 1° in the north. The middle and lower slopes show a relatively smooth surface morphology in the south and an irregular morphology in the northern area (Fig. 5). The base of the slope is located more proximal in the south relative to the north of the study area. The gradient of the basinal area is 0.3°–0.2° and it has a smooth morphology, particularly in the northern part (Fig. 5).

### Sea-floor morphological features

Several incisions are identified on the sea floor across the middle slope, particularly in the northern part of the study area. These are referred to as middle-slope channels and trend 30° ESE (Fig. 5). The middle-slope channels display a V-shaped cross-section about 200 km wide and 2 m deep, reaching water depths of nearly 1580 m. Larger incisions, also V-shaped and with the same orientation, are

identified across the northern part of the lower slope. These are referred to as lower-slope channels. The largest are 200 to 700 m wide and about 5 m deep (Fig. 5). They run over a distance of 3000 to 8000 m, ending in water depths of 1650 m. Both the middle- and lower-slope channels have an erosive character and are interpreted to have been formed by down-slope flows related to mass transport of sediments. Further incisions are identified in the southern basinal area. These are 350 m wide and 1.5 m deep and run over a distance of 2 km between water depths of 1658 and 1665 m (Fig. 5). They are interpreted to be distal channels, representing the most-oceanwards extent of down-slope flows, connected to the distal transport of sediments.

Two of the lower-slope channels end in small monticules (300 m across slope × 1000 m along slope) that stretch parallel to the slope, but generally the channels are located adjacent to vast lobe morphologies perpendicular to the margin at the base of the slope. The depositional lobes are particularly well developed in the northern part of the study area, where two major lobes are identified at the base of the slope (Fig. 5): the northern lobe is 3014 m wide and 3760 m long, while the southern lobe is 2160 m wide and 3110 m long (Fig. 5). Both depositional features, i.e. monticules and lobes, are interpreted to be associated with the deposition of sediments from down-slope mass transport. Considering the glacial nature of the study area, the erosive channels and depositional features are interpreted to be part of GDF systems.

Round-shaped depressions are identified on the southern lower slope. They show a U-shaped profile about 200 m wide and 5 m deep, and are concentrated in water depths of about 1500 m (Fig. 5). These depressions are interpreted as pockmarks according to Cathles *et al.* (2010), related to fluid and/or gas escape at the seabed, following migration through the sedimentary record.

Undulating seabed morphologies are identified at the base of the slope in the northern part of the study area and in the proximal basinal area (Fig. 5A). They are interpreted as sediment waves. The largest waves are 230 m wide and 4 m high, and sinuously extend over 2 km (Fig. 5). They are roughly parallel to slope contours and located

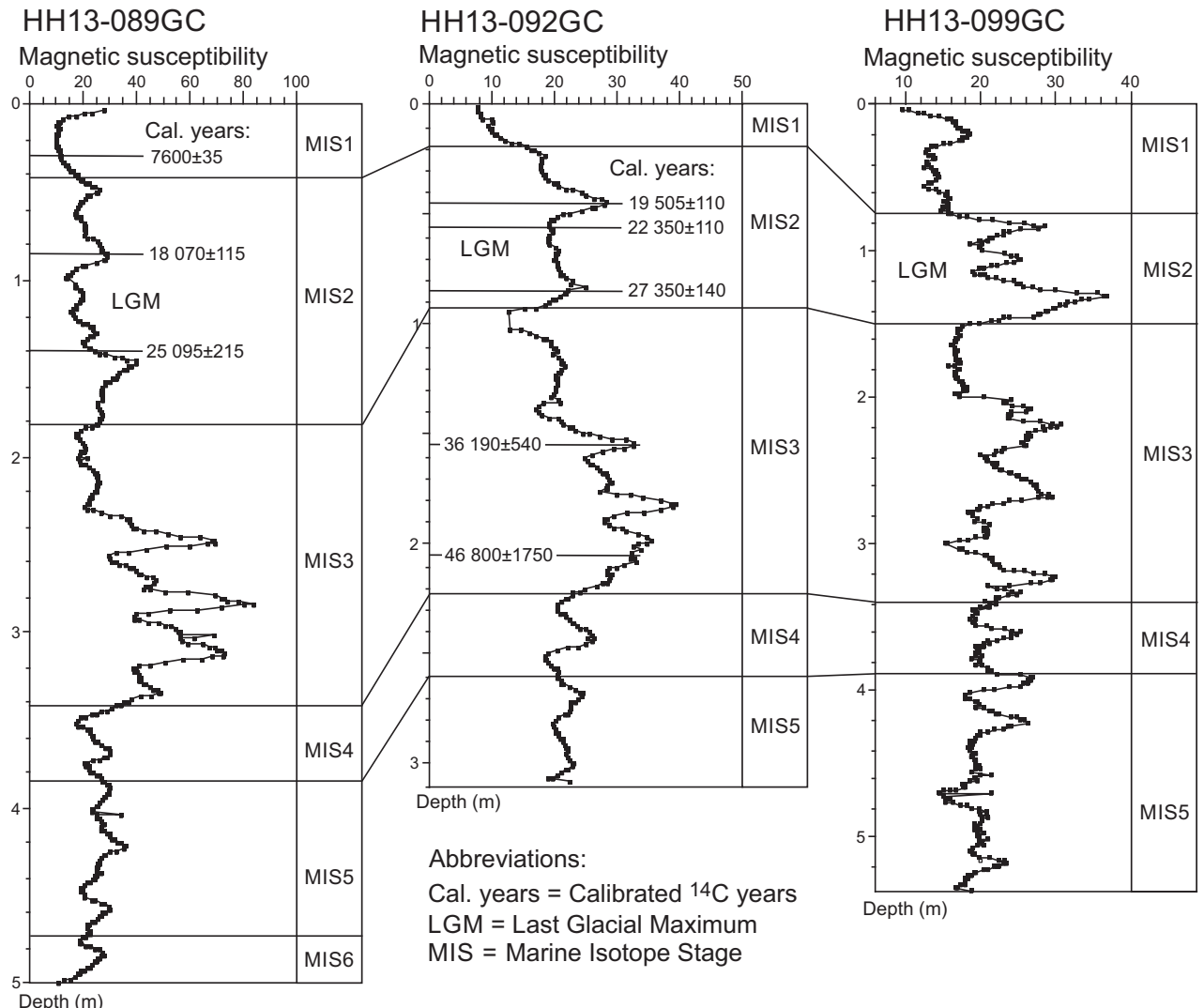


Fig. 4. Magnetic susceptibility (in  $10^{-5}$  SI units) curve of gravity cores HH13-099GC (1550 m water depth) compared to the magnetic susceptibility curves of HH13-092GC (1595 m water depth) and HH13-089GC (1616 m water depth; Gabrielsen 2017) and correlated with the Marine Isotope Stages (MIS). Note the location of 46.8 cal. ka age at 2.05 m deep discussed in the text. Location of the cores in Fig. 1.

between the lower-slope channels and the depositional lobes. These sediment waves are interpreted to be related to an across-slope flow, in agreement with Wynn & Stow (2002). In the proximal basinal area, the sediment waves are less pronounced, about 100 m wide and 1 m high and with straight or slightly sinuous crests. They are oblique to the margin and are particularly abundant along the southern part of the study area, where the longest extend about 3 km (Fig. 5). These sediment waves are interpreted to be related to the mobilization of sediments by along-slope currents according to Wynn & Stow (2002) and the classification of Stow *et al.* (2002).

#### Shallow sub-bottom features

Different acoustic facies are distinguished on the chirp sub-bottom profiles (Fig. 6). The middle and lower slope

is generally characterized by low-penetrative facies, with an irregular sea-floor reflection and few-to-no sub-bottom reflections (Figs 7A, 8A). We interpret these facies to be associated with MTDs (see above), formed by sediments moving down-slope from the continental shelf. The identified MTDs have a relatively transparent acoustic response and are interpreted as GDF deposits, formed by sediment instability generated by the oceanward advance of the ice sheet over the continental shelf.

The base of the northern slope is characterized by internal chaotic facies overlain by subparallel reflections with a wavy-irregular sea-floor expression, defined as ridge and valley topography (Figs 6, 7A, 8A), following the morphological nomenclature of García *et al.* (2012). Oceanwards, stratified and laterally continuous reflections are slightly tilted, forming a laminated body at about 1700 m water depth (Fig. 6). The laminated body

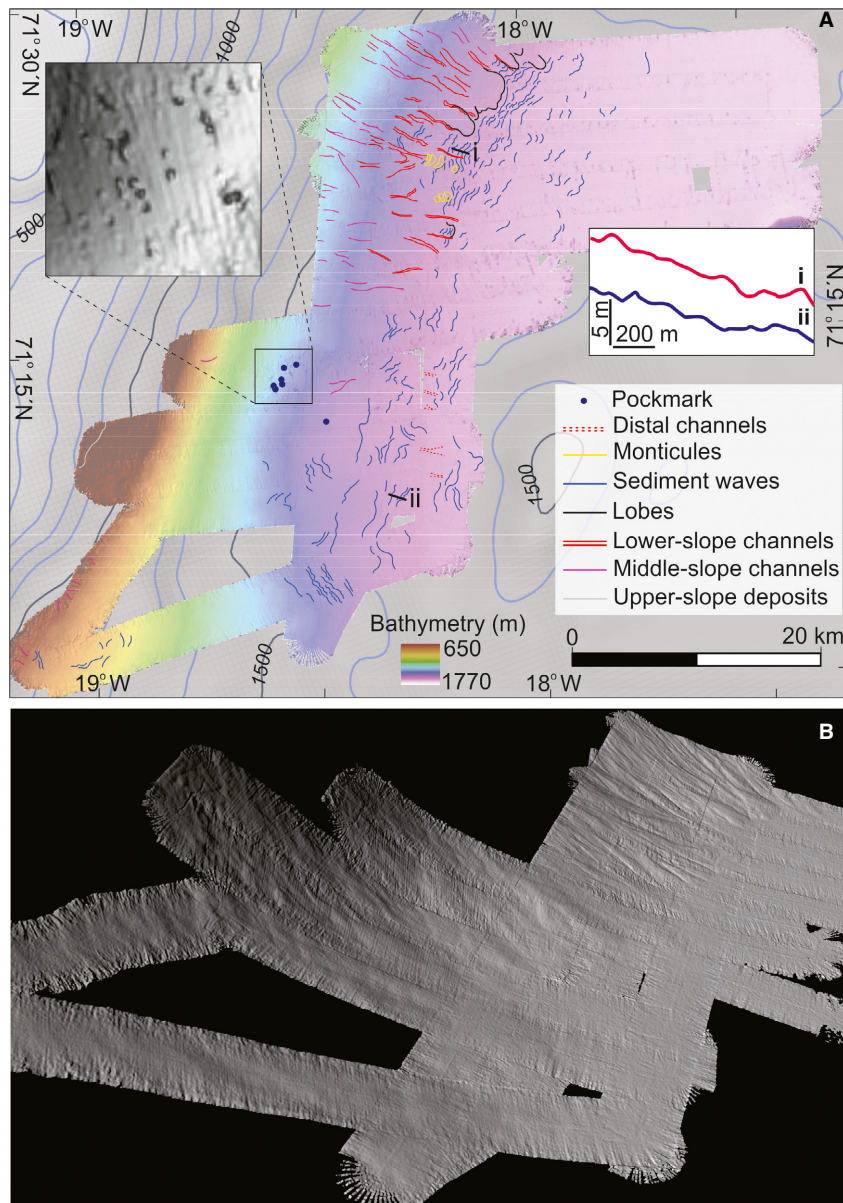


*Fig. 5.* Sea-floor features in the study area. A. Swath bathymetry map 30 × 30 m cell grid overlaying the International Bathymetric Chart of the Arctic Ocean (IBCAO, Jakobsson *et al.* 2012) bathymetry, with black isobaths every 500 m and blue isobaths every 100 m. Note the zoom over the pockmarks and the sea-floor profile over the sediment waves in the northern (i) and southern (ii) parts of the study area. B. Swath bathymetry data of the study area in an oblique view. [Colour figure can be viewed at [www.boreas.dk](http://www.boreas.dk)]

is interpreted as a plastered contourite drift, according to the classification established by Faugères *et al.* (1999) and Rebisco (2005). In the basinal area the plastered drift onlaps onto lateral continuous, undulating reflections that form a mounded body between 1725 and 1740 m water depth (Fig. 6). This body is interpreted to be a mounded contourite drift based on Faugères *et al.* (1999) classification.

The proximal area of the plastered drift displays an irregular surface over sub-bottom vertical structures (Fig. 6). Farther south, at the base of the slope, a similar pattern with horizontal and stratified reflections, dis-

rupted by scattered vertical fractures and underlain by MTDs, is identified (Fig. 8A). These structures are interpreted to have formed due to the migration of fluids through the upper sedimentary succession.

The southern base of the slope and basinal area is characterized by a generally stratified sub-bottom pattern of laterally continuous reflections that are slightly undulating (Figs 6B, 7A, 8A). Locally small transparent bodies with lenticular shapes (~800 m length and ~4 ms TWTT thick), considered to be small MTDs, are identified both on the sea floor and deeper in the stratified sedimentary record (Figs 6, 7A, 8A). Two pronounced

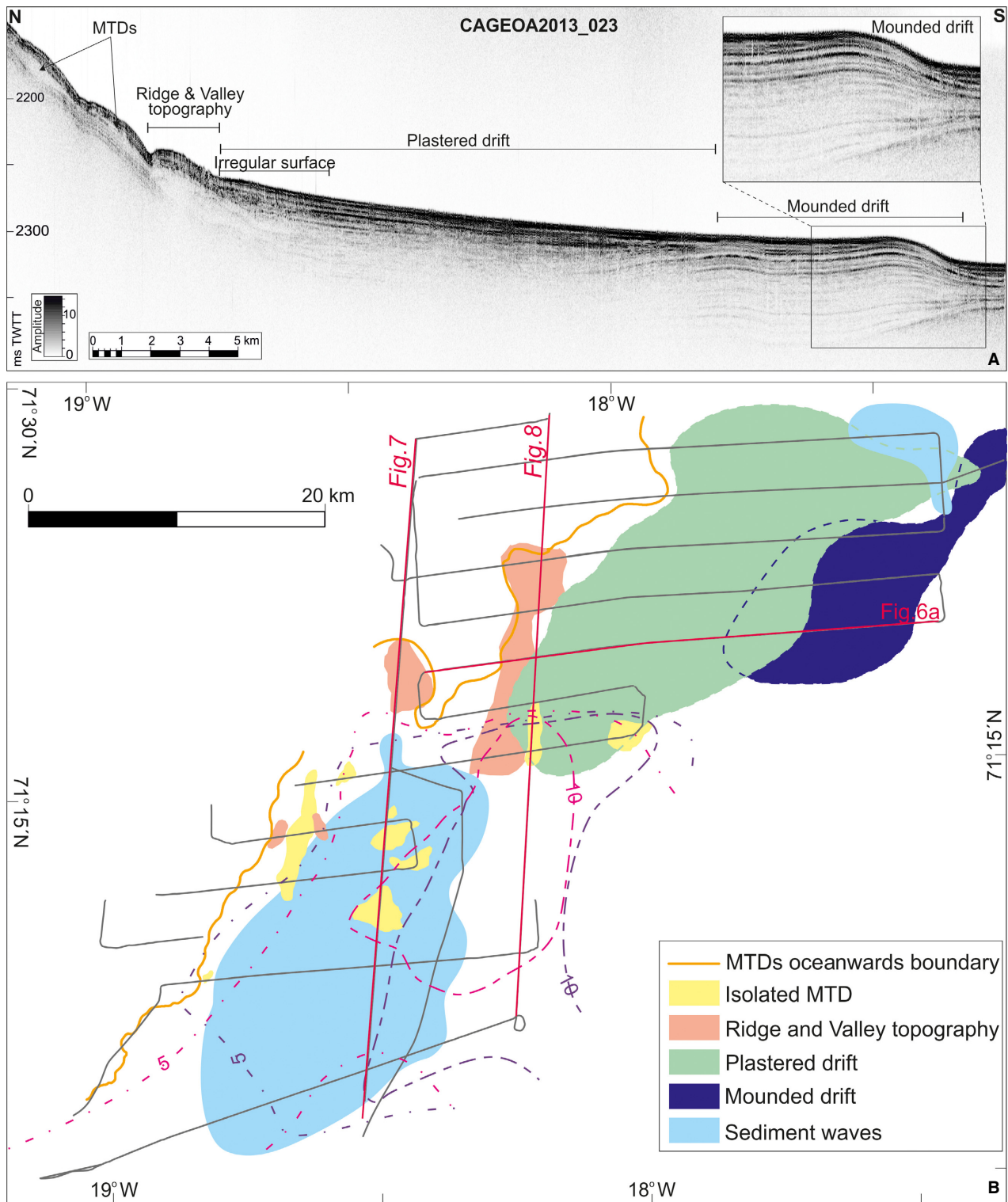


Fig. 6. Sub-bottom features. A. Chirp sub-bottom profile across the northern study area, see location in B. Notice the plastered and mounded drifts in the basinal area. Zoom over the mounded drift in the square. B. Distribution of the main features identified in the chirp sub-bottom profiles, the location of which is marked by the grey lines. Location of the chirp sub-bottom profiles in Figs 6A, 7 and 8 is shown. The purple and pink dotted lines show the distribution of the chirp units c2 and c1, respectively, thickness in ms two-way-travel-time (TWTT). [Colour figure can be viewed at [www.boreas.dk](http://www.boreas.dk)]

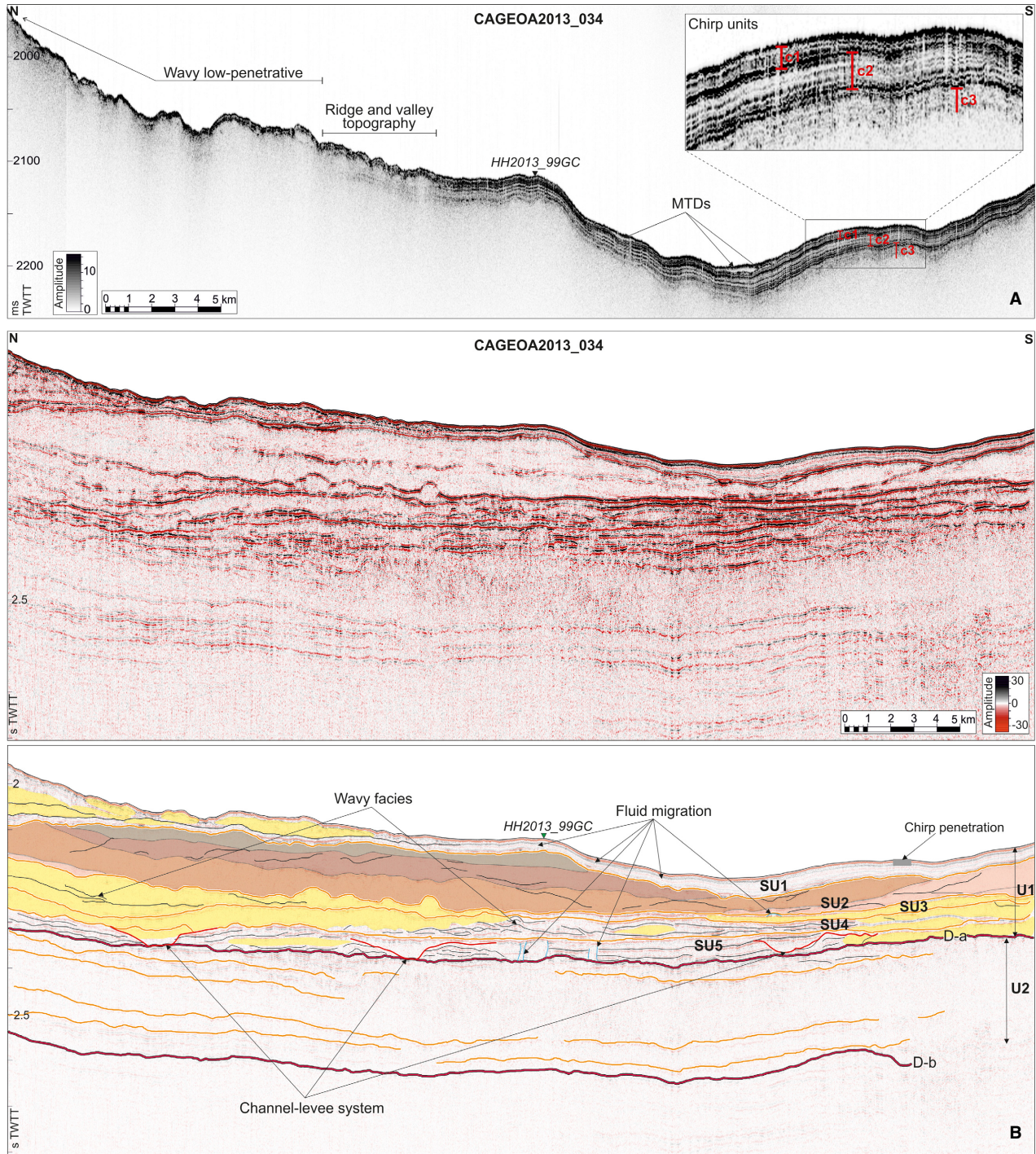


Fig. 7. Profile CAGE\_OA2013-034 along the lower slope of the study area. See location in Figs 1 and 6. A. Chirp sub-bottom profile. The main identified features are labelled. Detail of the chirp units in the square. B. High-resolution single-channel seismic profile: seismic signal (top) and interpretation (bottom). Discontinuities a and b are in red and minor discontinuities in orange. Mass transport deposit (MTD) bodies are shaded in yellow but those within SU2 are distinguished in different colours. The location of the gravity core HH2013\_99GC is shown. TWTT = two-way-travel-time. [Colour figure can be viewed at [www.boreas.dk](http://www.boreas.dk)]

acoustic reflections, together with a strong reflectivity variation, allow us to define three chirp units in the shallow sub-seabed section (Figs 7A, 8A). The lower chirp unit (c3) is characterized by high reflectivity that

decreases downwards. The base of c3 is not visible on the sub-bottom profiles. The middle chirp unit (c2) is characterized by low reflectivity (Figs 7A, 8A), and its thickness increases to the southwest with a maximum

along the proximal basinal area in the central and southern part of the study area (more than 20 ms TWTT thick; Fig. 5B). The upper chirp unit (c1) has high internal reflectivity and a maximum thickness (more than 20 ms TWTT) along the base of the slope in the central study area, thinning to the south (Figs 6B, 7A, 8A).

### *Seismic stratigraphy*

Seismic-stratigraphical analysis of the high-resolution seismic profiles allows us to distinguish major stratigraphical unconformities from the present sea floor down to 2.7 s TWTT depth (Figs 7B, 8B). Following the regional stratigraphical model published in Pérez *et al.* (2018), the sedimentary record is divided into two major seismic units (U2 and U1 from bottom to top) that are separated by a major regional unconformity called Discontinuity-a (Fig. 2). The seismic resolution of the lower seismic unit U2 is very low, forming a relatively homogeneous layer with few internal reflections; although to the north of the study area, reflections of low lateral continuity can be identified in its upper part (Figs 7B, 8B). The thickness of U2 varies from 285 ms TWTT along the northern lower slope to 200 ms TWTT along the base of the slope (Fig. 9A).

The distribution of the overlying seismic unit U1 is more heterogeneous, compared with U2. The thickness of the unit decreases southeastwards from 410 ms TWTT on the northern lower slope to 150 ms TWTT in the southern proximal basinal area, although the maximum thickness of 490 ms TWTT is located on the southern middle slope (Fig. 9A). The seismic resolution of U1 allows us to identify several stratigraphical features and to divide the unit into five subunits based on seismic facies variations. The subunits are named SU5 to SU1 from bottom to top, and are bounded by less distinct stratigraphical discontinuities that locally represent unconformities (Figs 7B, 8B).

The lowermost subunit (SU5) increases in thickness down-slope, from 32 ms TWTT along the lower slope to 100 ms TWTT at the base of the slope (Fig. 9A). Internal reflections within this subunit have relatively high lateral continuity and are organized in a stratified pattern (Fig. 8B). The stratified pattern is locally interrupted by vertical structures that indicate fluid migration through SU5 (Fig. 7B). Along the middle and lower slope the stratification is also interrupted by several zones of chaotic facies. These chaotic zones are formed by strong erosion – marked by erosive truncation of the reflections – that laterally continues into wavy reflections with low lateral continuity forming mound-shape bodies (Fig. 7B). These morphologies are interpreted to represent channel-levee complexes usually associated with turbidity currents (e.g. Mulder *et al.* 2008; Nelson *et al.* 2011). Along the southern base of the slope and basinal area the stratified pattern is replaced by sedimentary bodies with transparent to semi-transparent seismic

signatures interpreted as MTDs (Figs 7B, 8B). The maximum thickness of these bodies is 44.2 ms TWTT, located in the southeast basinal area (Fig. 8B). The combination of turbidity current-related features and MTDs is associated with GDF systems. However, in the southern part of the basinal area an erosive U-shaped zone continues laterally in a slightly mounded body, which is interpreted as a buried drift-moat system.

Above, subunit SU4 forms a thin layer, the thickness of which decreases from 62 ms TWTT along the lower slope to 22 ms TWTT in the southeastern base of the slope area (Fig. 9A). Internal reflections have a low lateral continuity and an undulating morphology, indicating sediment waves (Figs 7B, 8B). Several erosive areas, marked by truncations, are identified inside this subunit, particularly along the base of the slope (Fig. 8B). As within SU5, the reflection pattern of SU4 is also interrupted by MTDs. In the lower part of the unit they are interbedded within the generally stratified reflection pattern; however, widespread MTDs dominate the upper part of SU4 (Figs 7B, 8B). The maximum thickness of the MTDs is 50 ms TWTT. The stratified reflections at the northern base of the slope form a mounded body with northward progradation of the reflections, which resemble the morphology of a buried laminated or plastered drift (Fig. 8B).

Subunit SU3 has a maximum thickness along the northern lower slope (92 ms TWTT) (Fig. 9A), thinning towards the south (27 ms TWTT) and east, and disappearing in the northern base of the slope. Internally, this unit is represented by mostly transparent to semi-transparent facies with some areas of high amplitude reflections, laterally discontinuous in the central part of the study area (Figs 7B, 8B). MTDs are identified in particular along the northern lower slope where their thickness reaches 90 ms TWTT (Fig. 7B).

Subunit SU2 has highly variable thickness. It is thickest along the middle and lower slope, where it reaches 250 ms TWTT in the south and 151 ms TWTT in the north (Fig. 9A). Along the base of the slope it is only identified in the northern part, where its thickness reaches 76 ms TWTT. Internally SU2 comprises several large MTDs of highly variable thickness. These are bounded by a few high amplitude reflections with low lateral continuity (Figs 7B, 8B).

Subunit SU1 forms a thin upper layer. Its thickness increases from 20 to 200 ms TWTT on the central and northern lower slope, respectively (Fig. 9A), whereas it is more uniform along the base of the slope (over 40 ms TWTT). In the south, it presents a stratified pattern with slightly undulated, relatively lateral continuous internal reflections. Several MTDs disrupt the stratified pattern of the unit in the northern lower slope (Figs 7B, 8B). The thickness of the MTDs is about 40 ms TWTT. Vertical fractures and sediment mobilization features associated with fluid migration can be identified along the base of the slope (Fig. 7B).

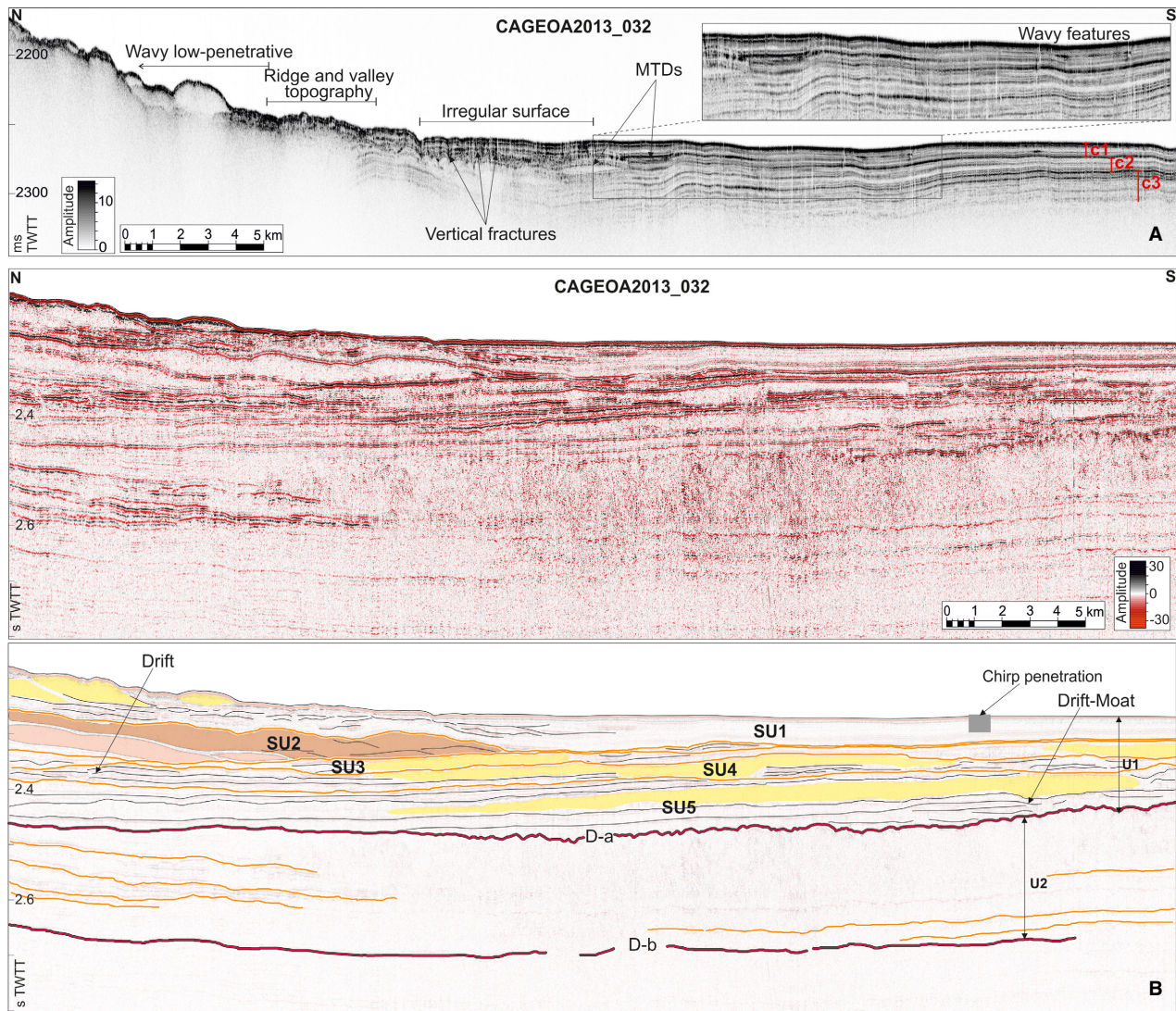


*Fig. 8.* Profile CAGE\_OA2013-032 along the base of the slope of the study area. See location in Figs 1 and 6. A. Chirp sub-bottom profile. The main identified features are labelled. Zoom over smooth wavy features in the square. B. High-resolution single-channel seismic profile: seismic signal (top) and interpretation (bottom). Discontinuities a and b are in red and minor discontinuities in orange. Mass transport deposit (MTD) bodies are shaded in yellow but those within SU2 are distinguished in different colours. TWTT = two-way-travel-time. [Colour figure can be viewed at [www.boreas.dk](http://www.boreas.dk)]

## Discussion

Most sedimentary processes identified off Liverpool Land, based on the results of this study, are observed within seismic unit U1, i.e. between the Discontinuity-a and the sea floor (Figs 7B, 8B). According to previously proposed stratigraphical models (see above) and the regional stratigraphical correlation (Fig. 2), this unit encompasses the Quaternary stratigraphical record from 1.6 Ma to the present (Fig. 3). The underlying seismic unit U2 potentially represents the early Quaternary period (2.05–1.6 Ma). Within the study area, the U1 sediment thickness increases northwards in contrast with the U2 sediment thickness that increases southwards. This indicates an overall

change in sediment distribution during the Quaternary (Fig. 9), which is interpreted to be related to a change in the prevalent sediment source, with sediments mainly delivered from the southern part of Liverpool Land during the early Quaternary and from the northern part of Liverpool Land during the late Quaternary.

### Cryospheric influence on the sedimentary processes

North of our study area, and associated with the Kejser Franz Joseph Fjord, four main phases of Quaternary GDF systems formation have been identified previous to this work (Wilken & Mienert 2006). Despite a common formation process, the GDF systems off Liverpool Land

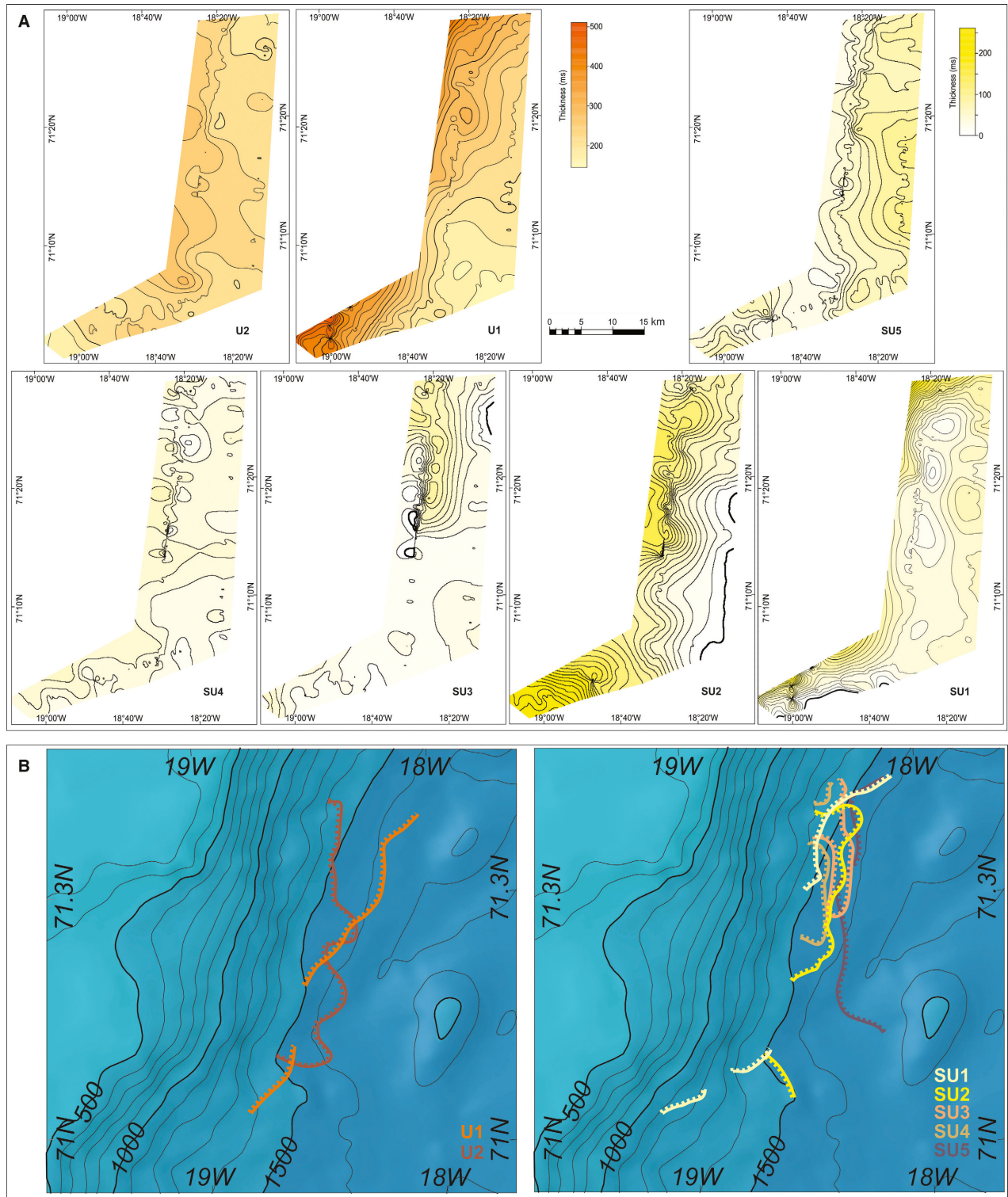


Fig. 9. A. Sediment thickness maps of the interpreted units and subunits in orange and yellow colours, respectively. B. Regional map with the major depocentres of the units and subunits highlighted. Note that the lines represent the boundaries of the depocentres. [Colour figure can be viewed at [www.boreas.dk](http://www.boreas.dk)]

have a stratigraphical distribution that differs from those described in the Kejser Franz Joseph Fjord area, as discussed below.

In the lowermost identified seismic subunit off Liverpool Land, SU5 (early Pleistocene age), buried turbiditic-channel systems along the lower slope

(Fig. 7B) led to the formation of buried GDF deposits at the base of the slope, predominantly observed in the southern part of the study area. This configuration points to a distal down-slope input from a glacial system in the Scoresby Sund area (Figs 7B, 8B, 9). The resulting GDF systems off Liverpool Land are related to ice streams flowing along the Scoresby Sund Fjord and crossing the continental shelf; a scenario that is consistent with the high sedimentation rates, drop-stones and sandy turbidites identified in ODP 987 (Jansen *et al.* 1996) and the large sediment input to the northern part of the Scoresby Sund TMF between 1.77 and 0.78 Ma (Laberg *et al.* 2013). The formation of the GDF systems identified in SU5 off Liverpool Land must have been triggered by grounded ice located on the outer shelf or at the shelf edge off Scoresby Sund. This is in contrast to the early Pleistocene system north of Kejser Franz Joseph Fjord described by Wilken & Mienert (2006), where the sedimentary record is characterized by an extensive deep-sea channel system and proximal formation of GDF deposits formed by an ice sheet located landwards of the shelf edge. The reduced extension of the ice sheet off Kejser Franz Joseph Fjord occurred during relatively warm conditions (Zhuravleva *et al.* 2017). The differences between the offshore sedimentary systems of Scoresby Sund and Kejser Franz Joseph during the early Pleistocene indicate a sedimentation pattern that suggests that the Greenland Ice Sheet extended farther across the continental shelf in the Scoresby Sund area compared to the northern East Greenland fjords (Fig. 10).

The number of GDF deposits off Liverpool Land increased during SU4 sedimentation in the mid-Pleistocene (Figs 3, 7B, 8B). We speculate that this upwards increase in GDF deposits occurred in line with the increase in global ice volume that accompanied the mid-Pleistocene transition (Head & Gibbard 2005; Laberg *et al.* 2018). This climatic shift took place between 0.9 and 0.92 Ma and represents the onset of the high amplitude 100-ka Milankovitch cycles, when precession-driven variations became more important (Berger & Wefer 1992; Raymo *et al.* 1997). The GDF deposits found in the southern part of subunit SU4 indicate an enhanced sedimentary input to the northern part of the Scoresby Sund TMF prior to 0.78 Ma. Some GDF deposits are also identified within SU4 in the northern part of the study area, pointing to the inception of an important ice stream through the northern fjord, i.e. Kong Oscar Fjord (Fig. 10). This change in the glacial stage of central-east Greenland during the mid-Pleistocene is also reflected in the significant change in the sedimentary pattern that occurred off Liverpool Land where the primary depocentres migrated landwards to the northern lower slope (Figs 7B, 8B, 9B). The northern glacial advance could have caused the decrease in the input of meltwater from the Greenland Ice Sheet to the eastern margin (Zhuravleva *et al.* 2017). The extension of the ice sheet to northern

Liverpool Land occurred at the time of the first identified GDF deposits on the North Sea Fan (1.1 Ma; Nygård *et al.* 2002), suggesting a regional increase in the activity of ice streams around the North Atlantic.

The two overlying subunits, SU3 and SU2, are mainly formed by large MTDs marking a dominant down-slope control on sedimentation off Liverpool Land (Figs 7B, 8B). We associate this down-slope deposition with the glacial intensification at 0.8 Ma, in agreement with grounded ice extending across the margin – tentatively to the shelf edge – that launched ice rafting of sediments eroded from the shelf and the formation of GDF deposits through sediment transport across the continental shelf and down the slope (Alley *et al.* 1989; Berger & Jansen 1994; Dowdeswell *et al.* 1997; Bart *et al.* 2000; Stokes *et al.* 2016; Laberg *et al.* 2018). Farther north of the study area, MTDs have likewise been related to full-glacial conditions and early stages of deglaciation (García *et al.* 2012). The internal distribution of the GDF deposits within SU3 and SU2 points to a changing sediment source through time (Fig. 10). While the lowest lying GDF deposits are more abundant in the southern part off Liverpool Land, and thus may have been generated by a southern source, the upper lying GDF deposits are more abundant in the northern study area, indicating a northern sediment source (Fig. 10). This distribution of the GDF deposits suggests that the activity of the Scoresby Sund ice-stream system decreased or diverted to the south, as the Kong Oscar Fjord ice-stream system activity increased, indicating a northward advance of the east Greenland cross-shelf glaciation.

The youngest seismic subunit, SU1, indicates a major change in the sedimentary pattern off Liverpool Land that occurred at about 0.4 Ma, according to the estimated age of this subunit (Figs 3, 4). The distribution of sediments, characterized by depocentres on the northern lower slope, and the southern stratified pattern of SU1 are taken as evidence of a lack of down-slope transport processes from the Scoresby Sund ice-stream system (Figs 7B, 8B, 9B). This is in agreement with the ice-raftered debris (IRD) trapped in the Scoresby Sund Fjord during the last 10 ka when only a minor amount of IRD reached the open shelf (Stein *et al.* 1993). However, the MTDs identified in the northern part of the study area indicate down-slope processes across the lower slope (Figs 7B, 8B). They may be related to advance of ice through Kong Oscar Fjord and across the continental shelf during the Saalian and Weichselian glacial periods (Hubberten *et al.* 1995). Farther north, moraines related to the maximum extent of the Greenland Ice Sheet during the LGM have also been identified on the mid-shelf off Kejser Franz Joseph Fjord (Evans *et al.* 2002). In addition, SU1 includes the period of maximum concentration of IRD in the upper continental slope in relation to the glaciation of the Jameson Land (Funder *et al.* 1998), when the ice sheet reached the mid-shelf (Funder

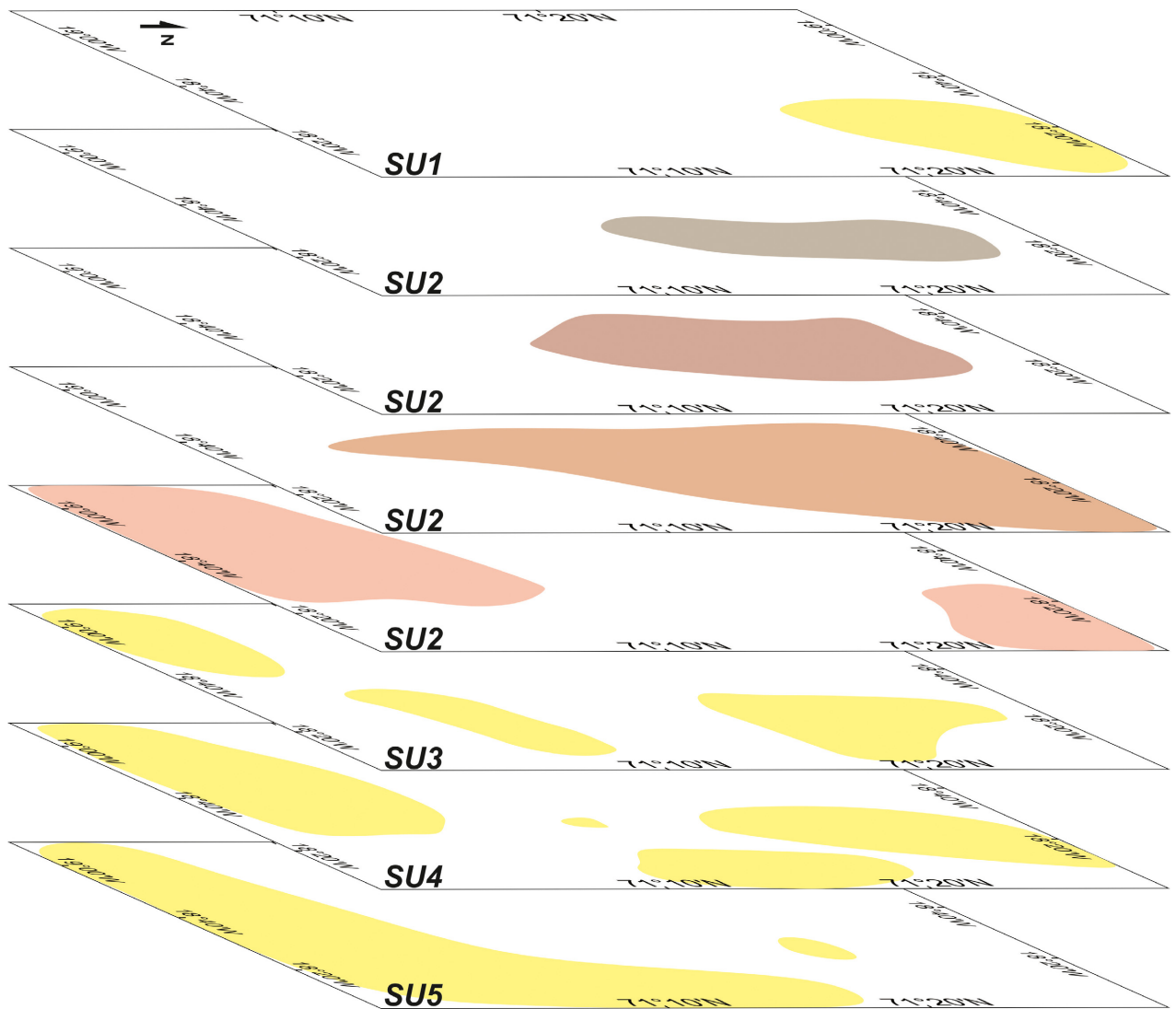


Fig. 10. Location of the major mass transport deposits (MTDs) identified in the sedimentary record as distinguished in the seismic profiles. The colour-scale of the distinguished MTD bodies follows Figs 7 and 8. Notice the northwards increase of MTDs upwards in the stratigraphic column. [Colour figure can be viewed at [www.boreas.dk](http://www.boreas.dk)]

*et al.* 1998; Evans *et al.* 2002); and the 0.2 Ma peak of GDF deposits along the east Greenland margin when the ice sheet last extended to the shelf edge (Wilken & Mienert 2006).

In addition to the differences in sedimentary processes between the two zones within SU1 distinguished off Liverpool Land, there are also clear morphological differences distinguishable on the sub-bottom profiles and swath bathymetry data (Figs 5, 6). There is no evidence of recent down-slope transport across the lower slope in the southern part of the study area, although it had occurred within the last 0.4 Ma. This is reflected in the stratified pattern of the chirp units (c1, c2 and c3) identified in the southern basinal area (Fig. 6B), i.e. at the northern Scoresby Sund TMF (Fig. 11), which is in accordance with observations by Ó Cofaigh *et al.* (2002). The differences in the down-slope sediment transport

activity off Liverpool Land may relate to the slightly steeper slope in the south compared with the northern part of the study area, which would support longer run-out distances oceanwards in the south. Thus, the gradient of the southern lower slope eases reworking of the MTDs into turbidity currents, evidenced by the distal channels in the basinal area (Fig. 5) and resulting in an effective by-passing across the slope (Pudsey & Camerlenghi 1998; Ó Cofaigh *et al.* 2003). In contrast, the channels, monticules and depositional lobes that form the GDF systems observed in the northern part of the study area provide evidence of down-slope sediment transport processes controlling the sedimentation and morphology of the middle and lower slopes (Figs 5, 6, 11), as occurred during the formation of SU1. This difference could denote a recent larger sediment input, or slope instability, in the northern part compared to the southern

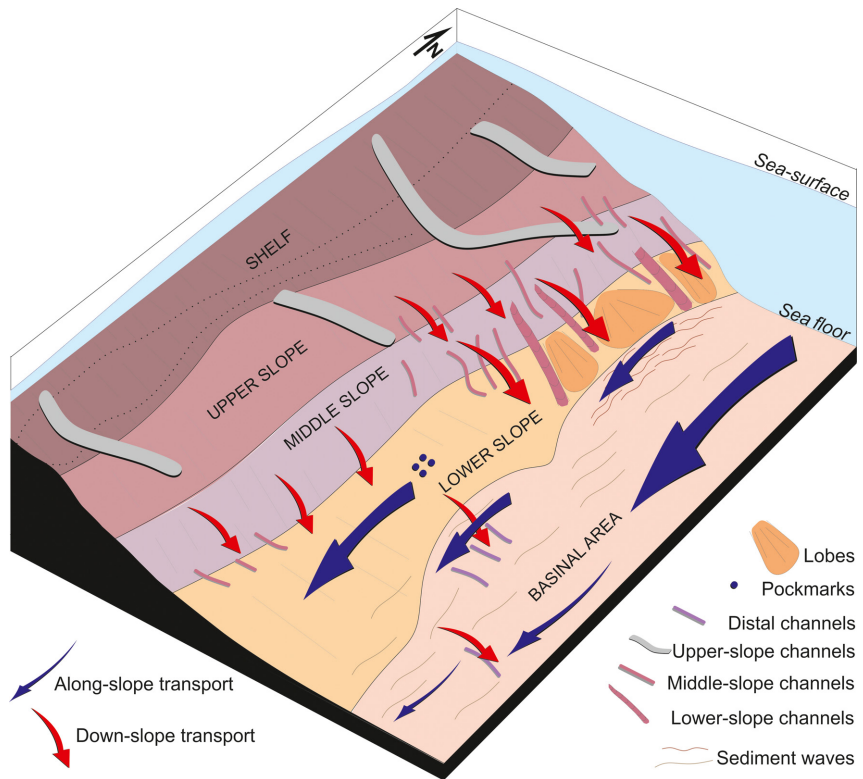


Fig. 11. 3D sketch of the central-east Greenland margin off Liverpool Land showing the main morphological features and dominating sedimentary processes. [Colour figure can be viewed at [www.boreas.dk](http://www.boreas.dk)]

part of the study area as discussed for SU1. The depocentres of the chirp units c2 and c1 reflect a northward migration, as occurred in the general trend of the discussed seismic units and subunits, supporting a northward relocation of the main sediment source along the Liverpool Land margin. However, the physiography of the slope is important as it determines the post-failure behaviour of the displaced sediments (Migeon *et al.* 2011). The gentle slope in the northern study area, where the continental shelf is also wider, makes it closer to the conceptual model of a classic TMF system (e.g. Polar North Atlantic; King *et al.* 1996, 1998; Dowdeswell *et al.* 1997; Vorren & Laberg 1997) where the fan formation occurred during glacial maxima (Ó Cofaigh *et al.* 2003). In this case, the sea-floor GDF systems observed off Liverpool Land may be related to the glaciations known as Scoresby Sund and Flakkerhuk (Funder *et al.* 1994, 1998), as are the depositional lobes described north of Kejser Franz Joseph Fjord (Wilken & Mienert 2006). In agreement with the GDF systems formed off Liverpool Land during the Quaternary, and discussed in the previous section, the TMFs would reach their maximum growth in the northern part of the study area during the maximum oceanwards location of the grounded ice sheet, whereas the morphology of the southern slope would favour a distal transport of sediments during ice-sheet stability periods.

#### Oceanographic influence on the sedimentary processes

A variety of current-related deposits, i.e. different kind of drifts and sediment waves, has been identified particularly along the base of slope and proximal basinal area off Liverpool Land. These current-related features are common at the sea floor and within the Quaternary sedimentary record, intercalated with the GDF systems. They may have been locally masked or eroded by other dominant processes, e.g. in SU3 and SU2 where the observed down-slope sedimentation may have removed potential current-related features (Figs 7B, 8B). The identified current-related features vary from drifts to wavy facies indicating action, to various degrees, of bottom currents over the sea floor at the time of deposition (Stow *et al.* 2002). The coexistence of current-related and glacial-related deposits identified in the geophysical data in this work reveals a cryospheric-oceanographic interaction in the construction of the central-east Greenland margin.

A buried drift-moat system is identified in SU5 in the southern basinal area of the study area indicating active along-slope bottom currents during the formation of the subunit. Based on its location and morphology (Fig. 8B), the system is interpreted to have been deposited by a bottom current similar to the present anti-clockwise flow of the GSDW in the southern Greenland Sea

(Jeansson *et al.* 2008). Thus, formation of this drift-moat system is suggested to involve GSDW convection in the Greenland Sea basinal area off Liverpool Land during the middle Pleistocene.

The presence of sediment waves and buried drifts observed at the base and lower slope slightly north in the study area within SU4 suggests an active bottom water flowing southwards along the slope (Figs 7B, 8B). The change in the character and location of the drifts from SU5 to SU4 suggests an apparent increase in along-slope current-related deposits. This could relate to the shift from intense, but zonal, oceanic circulation at high latitudes prior to the mid-Pleistocene transition, to meridional deep-water flows and major water-mass exchange with the North Atlantic, starting a strong overflow of bottom water from the Greenland Sea to the North Atlantic (Berger & Jansen 1994; Baumann & Huber 1999; Helmke *et al.* 2005). Even though there was suppression of NADW formation in the Greenland Sea during the mid-Pleistocene, this occurred together with an increased warm water advection and vigorous influx of oceanic heat to the Greenland Sea due to the progressive northward migration of the Arctic Front (Berger & Jansen 1994; Raymo *et al.* 1997; Henrich *et al.* 2002; Wright & Flower 2002).

The distribution and configuration of SU1 off Liverpool Land appears to have been controlled by the irregular morphology of the underlying unit. However, the undulating reflections observed along the southern lower slope and proximal basinal area suggest a slight influence of bottom-current activity (Fig. 7B). This is also supported by the slightly undulating signature of the reflections, which form the recent chirp units c1, c2 and c3 (Fig. 7B). The influence of bottom current in these areas is also revealed by the contourite drifts identified in the sub-bottom sedimentary records and the contourite-related sediment waves in the sea-floor morphology. The late Pleistocene onset of this bottom-current activity is in agreement with the reported increase in strength of glacial-related NADW formation from 0.4 Ma, even though the reasons for the increased production of NADW remain unclear (Raymo *et al.* 1997). The components of NADW did not vary significantly on glacial-interglacial time scales for most of the Pleistocene, thus deep-water formation north of the Denmark Strait continued although its production decreased during the LGM (Marchitto *et al.* 2002; Raymo *et al.* 2004).

The sediment waves identified at the southern lower slope and proximal basinal area off Liverpool Land are interpreted to be related to the activity of along-slope flows during the recent past and present margin history based on their morphology and distribution with respect to the margin (Fig. 5). However, the sediment waves identified at the base of the slope in the northern

part of the study area are interpreted as turbidity-related features in agreement with the interpretation of the sediment waves off the northeast Greenland margin (García *et al.* 2012). Contourite drifts are identified in the shallow sub-bottom and sea-floor records, particularly in the northern basinal area (Fig. 6). Both types of current-related deposits, i.e. sediment waves and contourite drifts, off Liverpool Land reveal relatively intense activity of along-slope bottom currents (Fig. 11). These bottom currents must be related to the EGC flowing southwards along the margin, but in the depth-domain of the GSDW. The observed differences in these features between the northern and southern parts off Liverpool Land could be associated with a vertical mixture of the GSDW with the above-flowing RAC (Jeansson *et al.* 2008), which would generate variations within the flow.

## Conclusions

The sedimentary processes observed along the slope off Liverpool Land reveal interaction between oceanographic and cryospheric processes in the construction of the margin during the Quaternary. While the oceanographic processes are mainly related to the southwards flow of the EGC and the formation of the GSDW within the Greenland Sea, the glacial influence on the margin is marked by the interaction between the various ice streams that originated from the main fjord systems of central-east Greenland. The southern ice stream associated with the Scoresby Sund glacial system was most active during the Pliocene and early-middle Pleistocene, while from the middle Pleistocene to the present day most of the down-slope sediment transport to the basinal area is related to the northern Kong Oscar Fjord glacial system. The abundance of glacial debris-flow deposits between 0.8 and 0.4 Ma points to ice streams reaching the shelf edge off Liverpool Land, whereas the northern ice streams reached the shelf edge off Kejser Franz Joseph Fjord only during the last 0.15 Myr according to Wilken & Mienert (2006). This northward migration in the formation of glaciogenic debrisflow systems and the oceanward ice-edge position confirm the northward migration of the glaciation along the central-east Greenland margin since the Early Pleistocene.

*Acknowledgements.* – The research developed for this work was performed under the GLANAM (GLAciated North Atlantic Margins) Initial Training Network FP7/2007-2013/ under REA grant agreement no 317217. We thank the Department of Geosciences at University of Tromsø (UiT) – the Arctic University of Norway – and Centre for Arctic Gas Hydrates, Environment and Climate (CAGE) for the personal and technical support during the initial development of the research, in particular Professor Karin Andreassen, T. L. Rasmussen and M. Winsborrow were supported by the Research Council of Norway through its Centres of Excellence Funding Scheme, project number 223259. We acknowledge the suggestions of D. Dove, M. García, J. Matthiessen and C. F. Forsberg that helped to improve the first version of the manuscript.

## References

- Aagaard, K., Coachman, L. K. & Institute of North America 21, N. 1968: The East Greenland Current II. *ARCTIC, Journal of the Arctic Institute of North America* 21, 267–290.
- Alley, R. B., Blankenship, D. D., Rooney, S. T. & Bentley, C. R. 1989: Sedimentation beneath ice shelves - the view from ice stream B. *Marine Geology* 85, 101–120.
- Bart, P. J., Anderson, J. B., Trincardi, F. & Shipp, S. S. 2000: Seismic data from the Northern basin, Ross Sea, record extreme expansions of the East Antarctic Ice Sheet during the late Neogene. *Marine Geology* 166, 31–50.
- Baumann, K. H. & Huber, R. 1999: Sea-surface gradients between the North Atlantic and the Norwegian Sea during the last 3.1 m.y.: comparison of Sites 982 and 985. *Proceedings of the Ocean Drilling Program: Scientific Results* 162, 179–190.
- Berger, W. H. & Jansen, E. 1994: Mid-Pleistocene climate shift - the Nansen connection. In Johannessen, O. M., Muench, R. D. & Overland, J. E. (eds.): *The Polar Oceans and Their Role in Shaping the Global Environment* 85, 295–311. American Geophysical Union, Washington D.C.
- Berger, D. & Jokat, W. 2009: Sediment deposition in the northern basins of the North Atlantic and characteristic variations in shelf sedimentation along the East Greenland margin. *Marine and Petroleum Geology* 26, 1321–1337.
- Berger, W. H. & Wefer, G. 1992: Neues vom Ontong-Java-Plateau (Westpazifik). *Naturwissenschaften* 79, 541–550.
- Butt, F. A., Elverhøi, A., Forsberg, C. F. & Solheim, A. 2001: Evolution of the Scoresby Sund Fan, central East Greenland - evidence from ODP Site 987. *Norsk Geologisk Tidsskrift* 81, 3–15.
- Cathles, L. M., Su, Z. & Chen, D. 2010: The physics of gas chimney and pockmark formation, with implications for assessment of seafloor hazards and gas sequestration. *Marine and Petroleum Geology* 27, 82–91.
- Channell, J. E. T., Smelror, M., Jansen, E., Higgins, S. M., Lehman, B., Eidvin, T. & Solheim, A. 1999: Age models for glacial fan deposits off East Greenland and Svalbard (Sites 986 and 987). *Proceedings of the Ocean Drilling Program: Scientific Results* 162, 149–166.
- Clausen, L. 1998: The Southeast Greenland glaciated margin: 3D stratal architecture of shelf and deep sea. *Geological Society, London, Special Publication* 129, 173–203.
- Døssing, A., Japsen, P., Watts, A. B., Nielsen, T., Jokat, W., Thybo, H. & Dahl-Jensen, T. 2016: Miocene uplift of the NE Greenland margin linked to plate tectonics: seismic evidence from the Greenland Fracture Zone, NE Atlantic. *Tectonics* 35, 257–282.
- Dowdeswell, J. A., Kenyon, N. H. & Laberg, J. S. 1997: The glacier-influenced Scoresby Sund Fan, East Greenland continental margin: evidence from GLORIA and 3.5 kHz records. *Marine Geology* 143, 207–221.
- Ehlers, B.-M. & Jokat, W. 2013: Paleo-bathymetry of the northern North Atlantic and consequences for the opening of the Fram Strait. *Marine Geophysical Research* 34, 25–43.
- Engen, Ø., Faleide, J. I. & Dyreng, T. K. 2008: Opening of the Fram Strait gateway: a review of plate tectonic constraints. *Tectonophysics* 450, 51–69.
- Evans, J., Dowdeswell, J. A., Grobe, H., Niessen, F., Stein, R., Hubberten, H.-W. & Whittington, R. J. 2002: Late Quaternary sedimentation in Kejser Franz Joseph Fjord and the continental margin of East Greenland. *Geological Society, London, Special Publications* 203, 149–179.
- Faugères, J. C., Stow, D. A. V., Imbert, P. & Viana, A. 1999: Seismic features diagnostic of contourite drifts. *Marine Geology* 162, 1–38.
- Funder, S., Hjort, C. & Landvik, J. Y. 1994: The last glacial cycles in East Greenland, an overview. *Boreas* 23, 283–293.
- Funder, S., Hjort, C., Landvik, J. Y., Nam, S. I., Reeh, N. & Stein, R. 1998: History of a stable ice margin - East Greenland during the middle and upper Pleistocene. *Quaternary Science Reviews* 17, 77–123.
- Gabrielsen, L. 2017: *Study of millennial scale paleoclimatic and paleoceanographic changes in conjunction with variations in the East Greenland Current during the late Quaternary*. M.Sc. thesis, the Arctic University of Norway (UiT), 155 pp.
- García, M., Dowdeswell, J. A., Ercilla, G. & Jakobsson, M. 2012: Recent glacially influenced sedimentary processes on the East Greenland continental slope and deep Greenland Basin. *Quaternary Science Reviews* 49, 64–81.
- Håkansson, L., Briner, J., Alexanderson, H., Aldahan, A. & Possnert, G. 2007: 10Be ages from central east Greenland constrain the extent of the Greenland ice sheet during the Last Glacial Maximum. *Quaternary Science Reviews* 26, 2316–2321.
- Hävik, L., Pickart, R. S., Väge, K., Torres, D., Thurnherr, A. M., Beszczynska-Möller, A., Walczowski, W. & von Appen, W. J. 2017: Evolution of the East Greenland Current from Fram Strait to Denmark Strait: synoptic measurements from summer 2012. *Journal of Geophysical Research: Oceans* 122, 1974–1994.
- Head, M. J. & Gibbard, P. L. 2005: Early-Middle Pleistocene transitions: an overview and recommendation for the defining boundary. *Geological Society, London, Special Publication* 247, 1–18.
- Helmke, J. P., Bauch, H. A., Röhl, U. & Mazaad, A. 2005: Changes in sedimentation patterns of the Nordic seas region across the mid-Pleistocene. *Marine Geology* 215, 107–122.
- Henrich, R., Baumann, K. H., Huber, R. & Meggers, H. 2002: Carbonate preservation records of the past 3 Myr in the Norwegian-Greenland Sea and the northern North Atlantic: implications for the history of NADW production. *Marine Geology* 184, 17–39.
- Hjort, C. 1973: A sea correction for East Greenland. *Geologiska Föreningens i Stockholm Förhandlingar* 95, 132–134.
- Hopkins, T. S. 1991: The GIN Sea-A synthesis of its physical oceanography and literature review 1972–1985. *Earth Science Reviews* 30, 175–318.
- Hubberten, H. W., Grobe, H., Jokat, W., Melles, M., Niessen, F. & Stein, R. 1995: Glacial history of East Greenland explored. *Eos* 76, 353–364.
- Jakobsson, M., Mayer, L., Coakley, B., Dowdeswell, J. A., Forbes, S., Fridman, B., Hodnesdal, H., Noormets, R., Pedersen, R., Rebisco, M., Schenke, H. W., Zarayskaya, Y., Accettella, D., Armstrong, A., Anderson, R. M., Bienhoff, P., Camerlenghi, A., Church, I., Edwards, M., Gardner, J. V., Hall, J. K., Hell, B., Hestvik, O., Kristoffersen, Y., Marcusen, C., Mohammad, R., Mosher, D., Nghiem, S. V., Pedrosa, M. T., Travaglini, P. G. & Weatherall, P. 2012: The International Bathymetric Chart of the Arctic Ocean (IBCAO) Version 3.0. *Geophysical Research Letters* 39, L12609, <https://doi.org/10.1029/2012gl052219>
- Jansen, E., Raymo, M. E. & Blum, P. 1996: *Proceedings, initial reports, Ocean Drilling Program, Leg 162, North Atlantic-Arctic gateways II*. 345–387. ODP, Texas A and M University, College Station.
- Japsen, P., Green, P. F., Bonow, J. M., Nielsen, T. F. D. & Chalmers, J. A. 2014: From volcanic plains to glaciated peaks: burial, uplift and exhumation history of southern East Greenland after opening of the NE Atlantic. *Global and Planetary Change* 116, 91–114.
- Jeansson, E., Jutterström, S., Rudels, B., Anderson, L. G., Olsson, A. K., Jones, E. P., Smethie, W. M. & Swift, J. H. 2008: Sources to the East Greenland Current and its contribution to the Denmark Strait Overflow. *Progress in Oceanography* 78, 12–28.
- King, E. L., Haflidason, H., Sejrup, H. P. & Løvlie, R. 1998: Glacigenic debris flows on the North Sea Trough Mouth Fan during ice stream maxima. *Marine Geology* 152, 217–246.
- King, E. L., Sejrup, H. P., Haflidason, H., Elverhøi, A. & Aarsæth, I. 1996: Quaternary seismic stratigraphy of the North Sea Fan: glacially fed gravity flow aprons, hemipelagic sediments, and large submarine slides. *Marine Geology* 130, 293–315.
- Knutz, P. C., Hopper, J. R., Gregersen, U., Nielsen, T. & Japsen, P. 2015: A contourite drift system on the Baffin Bay-West Greenland margin linking Pliocene Arctic warming to poleward ocean circulation. *Geology* 43, 907–910.
- Laberg, J. S., Forwick, M., Husum, K. & Nielsen, T. 2013: A re-evaluation of the Pleistocene behavior of the Scoresby Sund sector of the Greenland Ice Sheet. *Geology* 41, 1231–1234.
- Laberg, J. S., Rydningen, T. A., Forwick, M. & Husum, K. 2018: Depositional processes on the distal Scoresby Trough Mouth Fan (ODP Site 987): implications for the Pleistocene evolution of the Scoresby Sund Sector of the Greenland Ice Sheet. *Marine Geology* 402, 51–59.

- Laberg, J. S. & Vorren, T. O. 1995: Late Weichselian submarine debris flow deposits on the Bear Island Trough Mouth Fan. *Marine Geology* 127, 45–72.
- Larsen, H. C., Saunders, A. D., Clift, P. D., Beget, J., Wei, W., Spezzaferri, S. & ODP Leg 152 Scientific Party 1994: Seven million years of glaciation in Greenland. *Science* 264, 952–955.
- Marchitto, T. M. Jr, Oppo, D. W. & Curry, W. B. 2002: Paired benthic foraminiferal Cd/Ca and Zn/Ca evidence for a greatly increased presence of Southern Ocean Water in the glacial North Atlantic. *Paleoceanography* 17, 10–11.
- Mattingdal, R., Knies, J., Andreassen, K., Fabian, K., Husum, K., Grøsfjeld, K. & De Schepper, S. 2014: A new 6 Myr stratigraphic framework for the Atlantic-Arctic Gateway. *Quaternary Science Reviews* 92, 170–178.
- Migeon, S., Cattaneo, A., Hassoun, V., Larroque, C., Corradi, N., Fanucci, F., Dano, A., de Lepinay, B. M., Sage, F. & Gorini, C. 2011: Morphology, distribution and origin of recent submarine landslides of the Ligurian Margin (North-western Mediterranean): some insights into geohazard assessment. *Marine Geophysical Research* 32, 225–243.
- Mokeddem, Z. & McManus, J. F. 2016: Persistent climatic and oceanographic oscillations in the subpolar North Atlantic during the MIS 6 glaciation and MIS 5 interglacial. *Paleoceanography* 31, 758–778.
- Mulder, T., Faugères, J. C. & Gonthier, E. 2008: Mixed turbidite-contourite systems. *Developments in Sedimentology* 60, 435–456.
- Nelson, C. H., Escutia, C., Damuth, J. E. & Twichell, D. C. 2011: Interplay of mass-transport and turbidite-system deposits in different active tectonic and passive continental margin settings: external and local controlling factors. In Shipp, R. C., Weimer, P. & Posamentier, H. W. (eds.): *Mass-transport Deposits in Deepwater Settings*, 39–66. SEPM Society for Sedimentary Geology 96, Broken Arrow.
- Nielsen, T., De Santis, L., Dahlgren, K. I. T., Kuijpers, A., Laberg, J. S., Nygård, A., Praeg, D. & Stoker, M. S. 2005: A comparison of the NW European glaciated margin with other glaciated margins. *Marine and Petroleum Geology* 22, 1149–1183.
- Nielsen, T. & Kuijpers, A. 2013: Only 5 southern Greenland shelf edge glaciations since the early Pliocene. *Science Reports* 3, 1875, <https://doi.org/10.1038/srep01875>.
- Nygård, A., Sejrup, H. P., Haflidason, H. & King, E. L. 2002: Geometry and genesis of glaciogenic debris flows on the North Sea Fan: TOBI imagery and deep-tow boomer evidence. *Marine Geology* 188, 15–33.
- Ó Cofaigh, C., Dowdeswell, J. A., Evans, J., Kenyon, N. H., Taylor, J., Mienert, J. & Wilken, M. 2004: Timing and significance of glacially influenced mass-wasting in the submarine channels of the Greenland Basin. *Marine Geology* 207, 39–54.
- Ó Cofaigh, C., Taylor, J., Dowdeswell, J. A. & Pudsey, C. J. 2003: Palaeo-ice streams, trough mouth fans and high-latitude continental slope sedimentation. *Boreas* 32, 37–55.
- Ó Cofaigh, C., Taylor, J., Dowdeswell, J. A., Rosell-Melé, A., Kenyon, N. H., Evans, J. & Mienert, J. 2002: Sediment reworking on high-latitude continental margins and its implications for palaeoceanographic studies: insights from the Norwegian-Greenland Sea. *Geological Society of London, Special Publications* 203, 325–348.
- Parnell-Turner, R., White, N. J., McCave, I. N., Henstock, T. J., Murton, B. & Jones, S. M. 2015: Architecture of North Atlantic contourite drifts modified by transient circulation of the Icelandic mantle plume. *Geochemistry, Geophysics, Geosystems* 16, 3414–3435.
- Peyton, C. E. 1977: *Seismic Stratigraphy-Applications to Hydrocarbon Exploration*. 516 pp. American Association of Petroleum Geologists, Tulsa.
- Pérez, L. F., Nielsen, T., Knutz, P. C., Kuijpers, A. & Damm, V. 2018: Large-scale evolution of the central-east Greenland margin: new insights to the North Atlantic glaciation history. *Global and Planetary Change* 163, 141–157.
- Pickering, K. T. & Hiscott, R. N. 2016: *Deep Marine Systems. Processes, Deposits, Environments, Tectonics and Sedimentation*. 657 pp. AGU & Wiley, Oxford.
- Poore, H. R., Samworth, R., White, N. J., Jones, S. M. & McCave, I. N. 2006: Neogene overflow of Northern Component Water at the Greenland-Scotland Ridge. *Geochemistry, Geophysics, Geosystems* 7, Q06010, <https://doi.org/10.1029/2005gc001085>.
- Pudsey, C. J. & Camerlenghi, A. 1998: Glacial-interglacial deposition on a sediment drift on the Pacific margin of the Antarctic Peninsula. *Antarctic Science* 10, 286–308.
- Rasmussen, S., Lykke-Andersen, H., Kuijpers, A. & Troelstra, S. R. 2003: Post-Miocene sedimentation at the continental rise of Southeast Greenland: the interplay between turbidity and contour currents. *Marine Geology* 196, 37–52.
- Raymo, M. E., Oppo, D. W. & Curry, W. 1997: The Mid-Pleistocene climate transition: a deep sea carbon isotopic perspective. *Paleoceanography* 12, 546–559.
- Raymo, M. E., Oppo, D. W., Flower, B. P., Hodell, D. A., McManus, J. F., Venz, K. A., Kleiven, K. F. & McIntyre, K. 2004: Stability of North Atlantic water masses in face of pronounced climate variability during the Pleistocene. *Paleoceanography* 19, PA2008, <https://doi.org/10.1029/2003pa000921>.
- Reading, H. G. 1996: *Sedimentary Environments. Processes, Facies and Stratigraphy*. 688 pp. Blackwell Science, Cambridge.
- Rebesco, M. 2005: Contourites. In Richard, C., Selley, R. C., Cocks, L. R. M. & Plimer, I. R. (eds.): *Encyclopedia of Geology*, 513–527. Elsevier, London.
- Rebesco, M., Hernández-Molina, F. J., Van Rooij, D. & Wählén, A. 2014: Contourites and associated sediments controlled by deep-water circulation processes: state of the art and future considerations. *Marine Geology* 352, 111–154.
- Reimer, P. J., Bard, E., Bayliss, A., Beck, J. W., Blackwell, P. G., Bronk Ramsey, C., Buck, C. E., Cheng, H., Edwards, R. L., Friedrich, M., Grootes, P. M., Guilderson, T. P., Haflidason, H., Hajdas, I., Hatté, C., Heaton, T. J., Hoffmann, D. L., Hogg, A. G., Hughen, K. A., Kaiser, K. F., Kromer, B., Manning, S. W., Niu, M., Reimer, R. W., Richards, D. A., Scott, E. M., Southon, J. R., Staff, R. A., Turney, C. S. M. & van der Plicht, J. 2013: IntCal13 and Marine13 radiocarbon age calibration curves, 0–50,000 years cal BP. *Radiocarbon* 55, 1869–1887.
- Sarnthein, M. & Altenbach, A. V. 1995: Late Quaternary changes in surface water and deep water masses of the Nordic Seas and north-eastern North Atlantic: a review. *Geologische Rundschau* 84, 89–107.
- Sarnthein, M., Bartoli, G., Prange, M., Schmittner, A., Schneider, B., Weinelt, M., Andersen, N. & Garbe-Schönberg, D. 2009: Mid-Pliocene shifts in ocean overturning circulation and the onset of Quaternary-style climates. *Climate of the Past Discussions* 5, 269–283.
- Solheim, A., Faleide, J. I., Andersen, E. S., Elverhøi, A., Forsberg, C. F., Vanneste, K., Uenzelmann-Neben, G. & Channell, J. E. T. 1998: Late Cenozoic seismic stratigraphy and glacial geological development of the East Greenland and Svalbard-Barents sea continental margins. *Quaternary Science Reviews* 17, 155–184.
- Stein, R., Grobe, H., Hubberten, H., Marienfeld, P. & Nam, S. 1993: Latest Pleistocene to Holocene changes in glaciomarine sedimentation in Scoresby Sund and along the adjacent East Greenland Continental Margin: preliminary results. *Geo-Marine Letters* 13, 9–16.
- Stein, R., Nam, S. I., Grobe, H. & Hubberten, H. 1996: Late Quaternary glacial history and short-term ice rafted debris fluctuations along the East Greenland continental margin. *Geological Society of London, Special Publications* 111, 135–151.
- Stokes, C. R., Margold, M., Clark, C. D. & Tarasov, L. 2016: Ice stream activity scaled to ice sheet volume during Laurentide Ice Sheet deglaciation. *Nature* 530, 322–326.
- Stow, D. A. V., Faugeres, J. C., Howe, J. A., Pudsey, C. J. & Viana, A. R. 2002: Bottom currents, contourites and deep sea sediment drifts: current state-of-the-art. *Geological Society of London, Memories* 22, 7–20.
- Stuiver, M. & Reimer, P. J. 1993: Extended 14C database and revised CALIB radiocarbon calibration program. *Radiocarbon* 35, 215–230.
- Swift, D. A., Persano, C., Stuart, F. M., Gallagher, K. & Whitham, A. 2008: A reassessment of the role of ice sheet glaciation in the long-term evolution of the East Greenland fjord region. *Geomorphology* 97, 109–125.

- Thiede, J., Jessen, C., Knutz, P., Kuijpers, A., Mikkelsen, N., Nørgaard-Pedersen, N. & Spielhagen, R. F. 2010: Millions of years of Greenland ice sheet history recorded in ocean sediments. *Polarforschung* 80, 141–159.
- Tripathi, A. K., Eagle, R. A., Morton, A., Dowdeswell, J. A., Atkinson, K. L., Bahé, Y., Dawber, C. F., Khadun, E., Shaw, R. M. H., Shorttle, O. & Thamabala Sundaram, L. 2008: Evidence for glaciation in the Northern Hemisphere back to 44 Ma from ice rafted debris in the Greenland Sea. *Earth and Planetary Science Letters* 265, 112–122.
- Våge, K., Pickart, R. S., Spall, M. A., Moore, G. W. K., Valdimarsson, H., Torres, D. J., Erofeeva, S. Y. & Nilsen, J. E. Ø. 2013: Revised circulation scheme north of the Denmark Strait. *Deep Sea Research Part I: Oceanographic Research Papers* 79, 20–39.
- Vanneste, K., Uenzelmann-Neben, G. & Miller, H. 1995: Seismic evidence for long-term history of glaciation on central East Greenland shelf south of Scoresby Sund. *Geo-Marine Letters* 15, 63–70.
- Vorren, T. O. & Laberg, J. S. 1997: Trough mouth fans - Palaeoclimate and ice-sheet monitors. *Quaternary Science Reviews* 16, 865–881.
- Wilken, M. & Mienert, J. 2006: Submarine glacigenic debris flows, deep-sea channels and past ice-stream behaviour of the East Greenland continental margin. *Quaternary Science Reviews* 25, 784–810.
- Wolf, T. C. W. & Thiede, J. 1991: History of terrigenous sedimentation during the past 10 m.y. in the North Atlantic (ODP Legs 104 and 105 and DSDP Leg 81). *Marine Geology* 101, 83–102.
- Wright, A. K. & Flower, B. P. 2002: Surface and deep ocean circulation in the subpolar North Atlantic during the mid-Pleistocene revolution. *Paleoceanography* 17, 1068, <https://doi.org/10.1029/2002pa000782>.
- Wright, J. D. & Miller, K. G. 1996: Control of North Atlantic deep water circulation by the Greenland-Scotland Ridge. *Paleoceanography* 11, 157–170.
- Wynn, R. B. & Stow, D. A. V. 2002: Classification and characterisation of deep-water sediment waves. *Marine Geology* 192, 7–22.
- Zachos, J. C., Dickens, G. R. & Zeebe, R. E. 2008: An early Cenozoic perspective on greenhouse warming and carbon-cycle dynamics. *Nature* 451, 279–283.
- Zhuravleva, A., Bauch, H. A. & Van Nieuwenhove, N. 2017: Last Interglacial (MIS5e) hydrographic shifts linked to meltwater discharges from the East Greenland margin. *Quaternary Science Reviews* 164, 95–109.